



รายงานวิจัยฉบับสมบูรณ์

โครงการหินงอกจากประเทศไทยให้ข้อมูลเชิงลึกถึงความ แปรปรวนของลมมรสุมเอเชียตะวันตกเฉียงใต้

โดย อาจารย์ ดร.สกลวรรณ ชาวไชย ภาควิชาธรณีวิทยา คณะวิทยาศาสตร์ จุฬาลงกรณ์มหาวิทยาลัย

รายงานวิจัยฉบับสมบูรณ์

โครงการหินงอกจากประเทศไทยให้ข้อมูลเชิงลึกถึงความ แปรปรวนของลมมรสุมเอเชียตะวันตกเฉียงใต้

> อ.ดร. สกลวรรณ ชาวไชย ภาควิชาธรณีวิทยา คณะวิทยาศาสตร์ จุฬาลงกรณ์มหาวิทยาลัย

สนับสนุนโดยสำนักงานกองทุนสนับสนุนการวิจัยและ จุฬาลงกรณ์มหาวิทยาลัย

(ความเห็นในรายงานนี้เป็นของผู้วิจัย สกว.และต้นสังกัดไม่จำเป็นต้องเห็นด้วยเสมอไป)

บทคัดย่อ

รหัสโครงการ: MRG5980080

ชื่อโครงการ: โครงการหินงอกจากประเทศไทยให้ข้อมูลเชิงลึกถึงความแปรปรวนของลม

มรสุมเอเชียตะวันตกเฉียงใต้

ชื่อนักวิจัย: ดร.สกลวรรณ ชาวไชย

คณะวิทยาศาสตร์ จุฬาลงกรณ์มหาวิทยาลัย

E-mail Address: sakonvan.c@chula.ac.th

ระยะเวลาโครงการ: 2 ปี

การสำรวจหาถ้ำและหินงอกที่เหมาะสำหรับการศึกษาสภาพแวดล้อมและสภาพ ภูมิอากาศบรรพกาลเป็นเรื่องที่ท้าทายสำหรับนักวิทยาศาสตร์ ทั้งนี้การวิเคราะห์ธรณีเคมีและ ไอโซโทปของหินงอกที่มีการใช้อย่างแพร่หลายในการการศึกษาสภาพภูมิอากาศบรรพกาลจะใช้ เวลานานและเสียค่าใช้จ่ายสูงสำหรับการทำการทดลอง ดังนั้นการศึกษาเกี่ยวกับรูปร่างสัณฐาน ของหินงอกโดยไม่ทำลายตัวอย่าง จึงเป็นสิ่งจำเป็นเบื้องต้นเพื่อใช้ประโยชน์ในการเลือกตัวอย่าง หินงอกที่เหมาะสมสำหรับการศึกษาเชิงลึกและวิเคราะห์ด้วยเครื่องมือขั้นสูงต่อไป ในงานวิจัยนี้ ได้ทำการสำรวจถ้ำจำนวน 20 แห่ง ที่อำเภอบ้านไร่ จังหวัดอุทัยธานี ทางภาคตะวันตกของ ประเทศไทย โดยจากการสังเกตลักษณะทางกายภาพภายนอกของหินงอกที่เหมาะสมใน ภาคสนาม จากนั้นได้ทำการเก็บตัวอย่างหินงอกจากถ้ำน้ำ จำนวน 3 ตัวอย่าง เพื่อใช้ทดสอบ คุณสมบัติของหินงอกสำหรับงานวิจัยเกี่ยวกับการเปลี่ยนแปลงสภาพภูมิอากาศบรรพกาล โดย ในขั้นตอนแรกได้นำตัวอย่างหินงอกไปสแกนโดยเครื่องเอกซ์เรย์คอมพิวเตอร์ (CT scanning) และนำภาพที่ได้จาก CT scan ไปมาเปรียบเทียบกับลักษณะศิลาวรรณาของหินงอกหลักจาก การตัดหินทดสอบ พบว่าลักษณะโครงเนื้อหิน (fabric) แบบ Columnar มีความหนาแน่นสูงสุด ในขณะที่โครงเนื้อหินแบบ dendritic แบบปิดและแบบเปิด มีความหนาแน่นปานกลางและต่ำสุด ตามลำดับ จากนั้นได้ทำหาอายุการสะสมตัวของหินงอกโดยวิธี U-Th dating พบว่าหินงอกทั้ง สามตัวอย่างนี้มีอายุสะสมตัวอยู่ในช่วง ~ 87,000 และ ~ 105,000 ปีก่อนปัจจุบัน ซึ่งจัดเป็นหิน งอกที่เก่าแก่ที่สุดที่เคยมีการรายงานในพื้นที่เอเชียตะวันออกเฉียงใต้ อย่างไรก็ตามลักษณะทาง กายภาพบ่งชี้ว่าหินงอกนี้มีกระบวนการเปลี่ยนแปลงหลังการสะสมตัว และกระบวนการแปรรูป ใหม่ ซึ่งส่งผลต่อสมบัติทางเคมีของหินงอก ดังนั้นจึงไม่เหมาะสมสำหรับการวิจัยเกี่ยวกับสภาพ ภูมิอากาศในอดีต ทั้งนี้ลักษณะเฉพาะของการเปลี่ยนแปลงนี้ไม่สามารถระบุได้ด้วยการ ตรวจสอบด้วยสายตาโดยไม่ตัดชิ้นส่วนหินงอก การศึกษานี้แสดงให้เห็นว่าภาพจาก CT scan สามารถใช้ประโยชน์ในการระบุลักษณะศิลาวรรณาของหินงอก โดยเฉพาะในการแยกประเภท หินงอกที่มีโครงเนื้อหินที่มีความเป็นรูพรุนและความหนาแน่นต่ำ ซึ่งคุณสมบัติดังกล่าวสามารถ ช่วยในการเลือกระนาบที่เหมาะสำหรับการตัดหินเพื่อแยกชิ้นส่วนและเพิ่มโอกาสในการศึกษา หินงอกเพื่อประโยชน์ทางด้านการเปลี่ยนแปลงสภาพภูมิอากาศให้ที่มีประสิทธิภาพมากขึ้น คำหลัก: หินงอก ภาคตะวันตกของประเทศไทย การเปลี่ยนแปลงสภาพภูมิอากาศบรรพกาล

Abstract

Project Code: MRG5980080

Project Title: Thai stalagmites give insight into southwest monsoon

variability

Investigator: Dr. Sakonvan Chawchai

Department of Geology, Chulalongkorn University

E-mail Address: sakonvan.c@chula.ac.th

Project Period: 2 years

Locating suitable caves and stalagmites for palaeoenvironmental and palaeoclimatic studies can be challenging. Isotopic geochemical analyses, albeit commonly performed for palaeoclimatic reconstruction, are also time consuming and costly. Therefore, petrographic and non-destructive morphological studies on speleothems become desirable to facilitate sample selection for further analysis. In this study, twenty caves were surveyed at Ban Rai district, Uthai Thani province in western Thailand. After external physical observations in the field, three stalagmite samples were collected from Tham Nam Cave to test their potential for palaeoclimatic research. Firstly, the stalagmites were scanned by X-ray computed tomography (CT scanning), and the CT images were subsequently compared with petrographic inspections. Columnar fabrics show the highest density, whereas closed and open dendritic fabrics indicate medium and the lowest densities, respectively. Layers near the top and bottom of the three stalagmites were dated by U-Th mass spectrometric techniques. All three samples were deposited between ~87 and ~105 ka ago; therefore, they are probably the oldest stalagmites that have been reported so far from mainland Southeast Asia. However, their physical features indicate that all the samples have suffered from post-depositional dissolution, and are unlikely suitable for palaeoclimatic research. The internal dissolution feature of stalagmites, however, cannot be identified by visual inspection of uncut samples. We hereby argue that CT images are useful to characterize stalagmite petrography, in particular fabric, porosity and density. Such features can be used to select the ideal plane of a stalagmite for sectioning, and then to maximise the chances of robust climatic reconstruction.

Keywords: Stalagmite, Western Thailand, Paleoclimate

Executive Summary

1. Introduction

Speleothems are secondary carbonate deposits formed inside caves. Their fabrics, stable isotope ratios, trace element compositions and organic chemistry can record events that occur at the cave surface during their growth history (McDermott 2004; Fairchild et al. 2006). Several types of speleothems (e.g., flowstones, stalactites and stalagmites) have been used as palaeoenvironmental and palaeoclimatic archives to study the changes of local or regional temperature, vegetation and precipitation, thanks to their continuous or semi-continuous deposition, absolute and precise datability, occurrence over a wide range of latitudes and possible conservation of palaeoclimate signals on millennial, decadal and even annual time scales (e.g. Hendy 1971; Banner et al. 2004; McDermott 2004; Fairchild et al. 2006; Fairchild & Treble 2009; Lachniet 2009; Mickler et al. 2014; Wong & Breecker 2015). Stalagmites have been favorably used in past hydroclimate reconstruction because of their predominantly column shapes and relatively simple sequential depositions (e.g. Zhang et al. 2008; Cai et al. 2010; Chen et al. 2015; Sinha et al. 2015). However, it remains a challenge to find suitable caves and stalagmite samples for palaeoclimatic research because only pristine stalagmites, deposited under chemical equilibrium conditions, can faithfully record climate signals.

Mainland Southeast Asia (e.g., Thailand, Myanmar, Malaysia peninsula and Laos) is strategically located on the route of moisture transport of the Indian summer monsoon (ISM, Fig. 1A). The agrarian societies dominant in the region heavily rely on the monsoon rainfall. Changes in rainfall intensity and variability therefore have a great impact on people's livelihoods in mainland Southeast Asia (Loo *et al.* 2015). The projection of future hydroclimate change in the region demands a good understanding of monsoon rainfall history (Cook *et al.* 2010; Raghavan *et al.* 2017; Thirumalai *et al.* 2017). Instrumental records of precipitation and temperature are however short (<50 years) and sparse in mainland Southeast Asia. Hence, palaeoclimate proxy data have to be applied to delineate the natural variability as well as anthropogenic contribution of climate change. Yet, such studies are still scarce in mainland Southeast Asia.

The beauty of the caves and speleothems in mainland Southeast Asia has attracted millions of tourists and visitors from around the world. Stalagmites from this

region however have rarely been investigated for palaeoenvironmental research. In Thailand for instance, only two stalagmite records have been reported so far. In these studies, stalagmites from the Namjang Cave, Mae Hong Son province in northwestern Thailand (Fig. 1A) were used to reconstruct monsoon variability covering the last 1700 and 400 years, respectively (Cai *et al.* 2010; Muangsong *et al.* 2014). Stalagmite growth rates during the last century from Namjang have been correlated with meteorological data, showcasing the potential palaeoclimatic proxy of Thailand monsoon rainfall (Muangsong *et al.* 2014).

In recent years, there have been studies on diagenetic alteration (e.g., dissolution, recrystallization and neomorphism) in speleothems. This process results in resetting chemical properties in samples, and they can no longer represent the original depositional conditions (Perrin *et al.* 2014; Scholz *et al.* 2014; Zhang *et al.* 2014; Bajo *et al.* 2016). The diagenetic alteration of speleothems can be observed through analysing petrography, internal microstratigraphy and trace elements in samples (Frisia *et al.* 2002; Railsback *et al.* 2002). These petrographic and non-destructive morphological studies are important to evaluate speleothems before further chemical analysis.

X-ray computed tomography (CT scanning) is a non-destructive technique for visualizing interior features of opaque solid objects by measuring the intensity of X-rays when they pass through the objects. The principle of computed tomography is to acquire multiple sets of views of an object over a range of angular orientations. These data are used to create two-dimensional images that are called slices (along the scan plane) and then provide a three-dimensional image of a volume by obtaining a series of contiguous slices (Ketcham & Carlson 2001). CT scanning has previously been used in studying speleothem features, including porosity (Mickler *et al.* 2004), macroholes and post-depositional off axis holes (Zisu *et al.* 2012), and calcite density (Vanghi *et al.* 2015; Walczak *et al.* 2015), as well as in exploring evidence of diagenesis in speleothems (Bajo *et al.* 2016). It has been proposed that CT images of uncut stalagmites can provide essential information of petrography to evaluate the potential impact on U-Th ages and isotopic geochemical analyses, which cannot be visually identified instead.

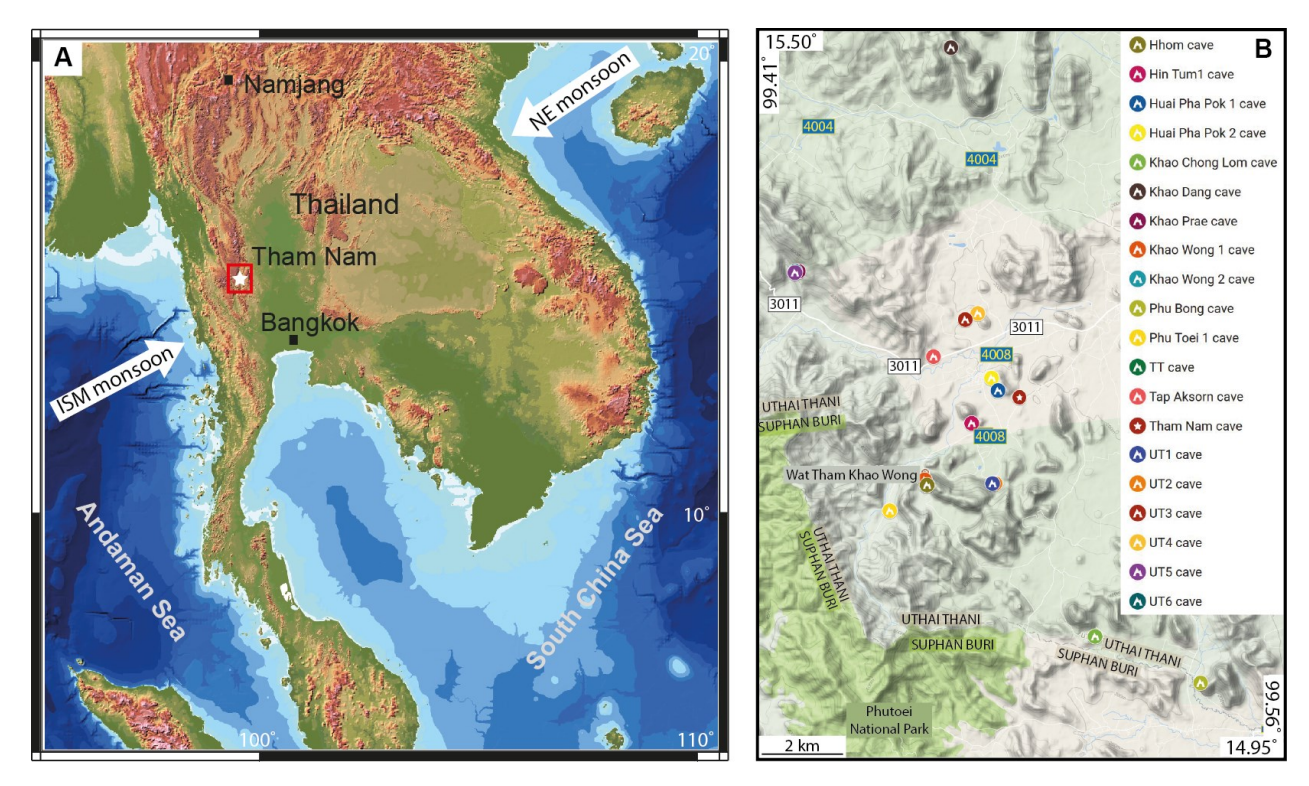


Fig. 1A. Locations of Ban Rai district (red square) and Tham Nam Cave (white star) in Uthai Thani, western Thailand. B. Locations of surveyed twenty caves in Ban Rai, Uthai Thani province.

The aim of this study is to find stalagmite samples in Ban Rai district, Uthai Thani province, western Thailand (Fig. 1A and B), based on their external physical properties (e.g. shape, color and texture), and analyse them with respect to their potential for paleaoclimatic research via CT scanning, petrographic studies, and U-Th analysis.

2. Materials and methods

Geological setting

The study area is located in national parks and national conservation zones of the Ban Rai district, Uthai Thani province, western Thailand (Fig. 1A, B). All caves in this area are overlain by host rock of argillaceous limestone, which is of Ordovician age indicated by fossil nautilus and crinoids (Department of Mineral Resources (DMR) 2009).

In this study, twenty caves were explored (Fig. 1A, B). Fifteen of them do not contain any stalagmites; three caves contain broken stalagmites that show visible macro-holes and irregular external surfaces; and the other two caves contain both broken and standing stalagmites. Based on their external features (nearly symmetrical,

column shapes, no obvious corrosions), three standing stalagmite samples (BR1, BR2 and BR3) were collected from Tham Nam Cave, a 300 m-long cave (15.05° N, 99.48° E; 200 m a.s.l; Fig. 1A, B). The stalagmites were retrieved from a large chamber \sim 200 m from the cave entrance.

Climate in western Thailand is mainly influenced by the ISM, which brings in torrential rains from the Bay of Bengal. Additional precipitation can be contributed by tropical cyclones from the South China Sea in the east during the summer. Mean annual rainfall in Uthai Thani province is about 1770 mm with 105 rain days on average. Mean annual temperature is around 28° C (data from Thai Meteorological Department, AD 1962-2015).

X-ray computed tomography (CT scanning) and petrography

Firstly, the stalagmites BR1, BR2 and BR3 (Fig. 2) were scanned with X-ray computed tomography (CT scanner) at King Chulalongkorn Memorial Hospital, Bangkok, Thailand. The X-ray computed tomography (GE Discovery 750 HD) was operated at a tube voltage of 140 kV and a current intensity of 80 mA. The CT scanner was set to a 0.625 mm slice thickness, with a 0.4 mm overlay between slice spacing. Reconstructed images were exported as Digital Imaging and Communications in Medicine (DICOM) files.

When X-rays scan an object, a portion of the radiation can be absorbed or reflected. Such interaction between the X-rays and the object is dependent upon the X-ray energy and the atomic structures of the object. The rest of X-rays that pass through the sample are collected by a detector, which converts them into light radiations. The light radiations are then transformed by a digital camera and later processed by a computer into images (Ketcham & Carlson 2001).

CT numbers in Hounsfield Units (HU) define the intensity of the transmitted X-ray beam. The HU is calculated from the relative value of the linear voxel attenuation coefficient (µvoxel) normalized to the reference material water (µwater), which is then multiplied by a magnifying integer constant (Mickler *et al.* 2004):

CT numbers in Hounsfield Units (HU) = $K [(\mu voxel-\mu water)/\mu water]$.

CT image processing and data analysis were performed using MeVisLab 2.6.2 software (http://www.mevislab.de/). CT images are shown both in colour images (Fig. 2B) and greyscale (Fig. 3) of axial sections, which are related to stalagmite's density (Mickler *et al.* 2004; Vanghi *et al.* 2015; Walczak *et al.* 2015). In greyscale, the

denser the scanned stalagmites, the brighter the images in CT slices (Fig. 3).

After CT scanning, the plane along the growth axis with less variability in density was chosen for sectioning, and the samples were cut to characterize and describe the different fabrics of the stalagmites. Based on different CT numbers (HU), nineteen polished thin sections were made (Fig. 3).

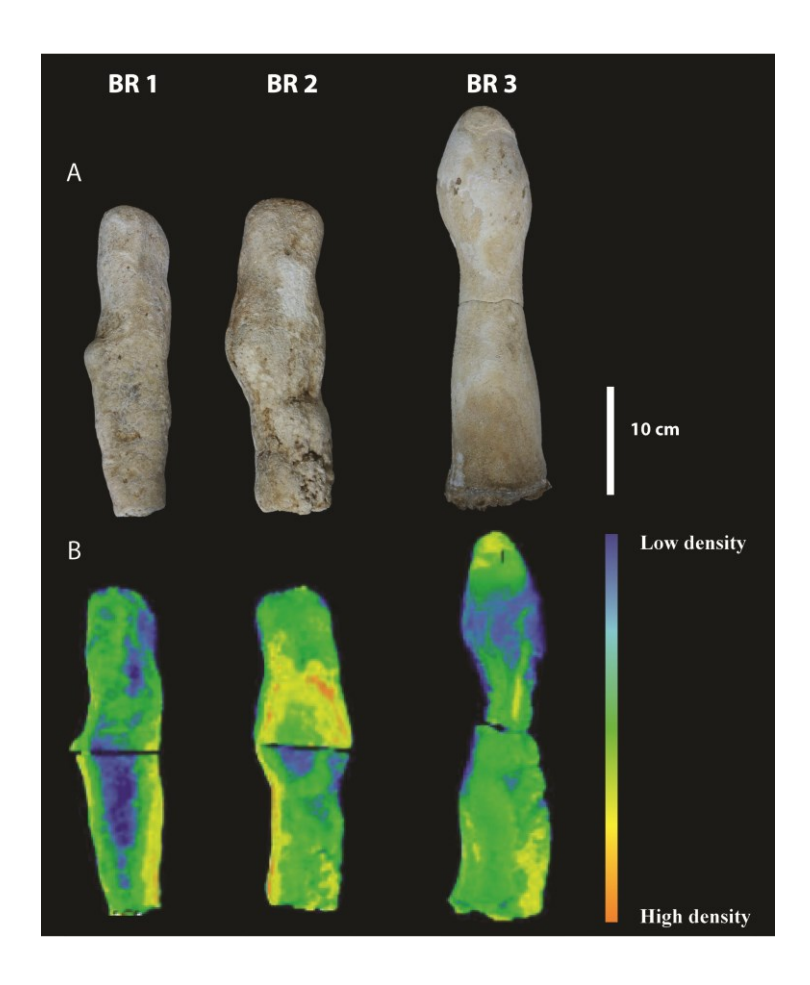


Fig. 2A. Stalagmite samples BR1, BR2 and BR3. B. 2D images of the stalagmites from CT scanning (colour scale: blue colour represents the lowest density; green colour indicates medium density and red/orange colours represent highest density).

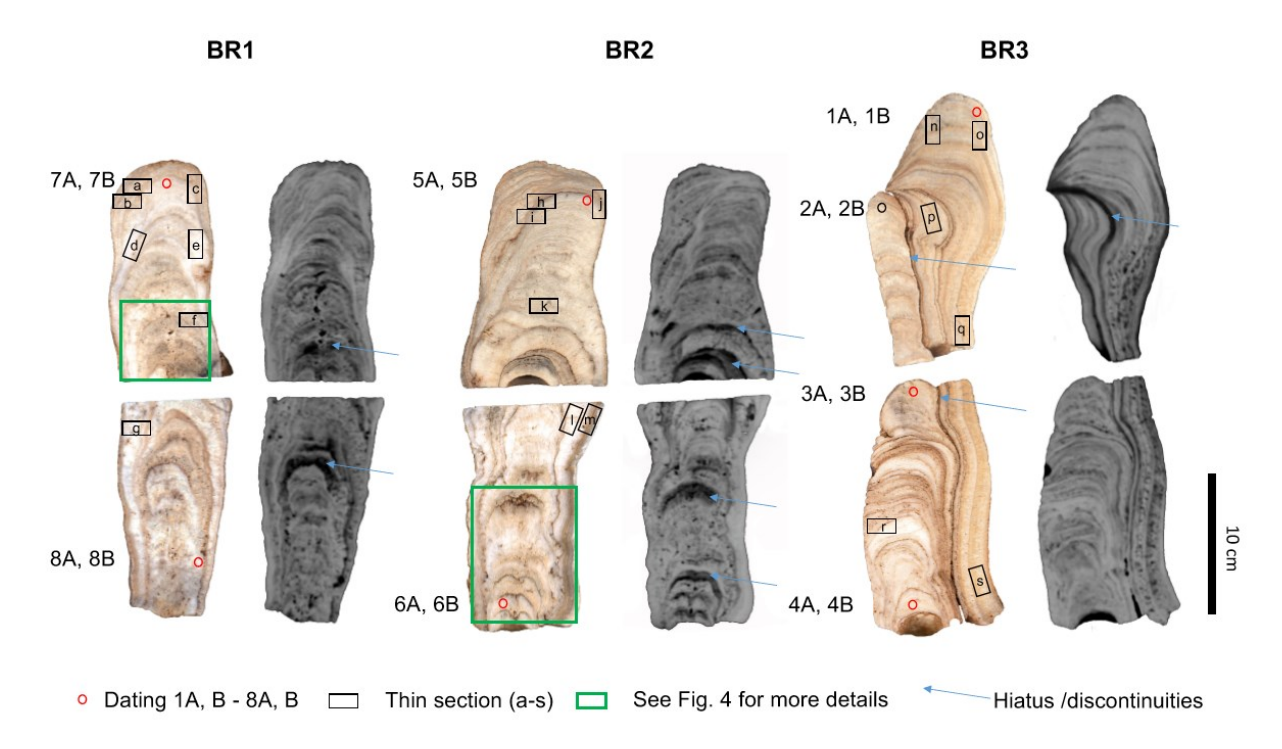


Fig. 3. Halved sections of stalagmite BR1, BR2 and BR3 compared to 2D images of uncut sample from CT scanning in greyscale. Higher densities are indicated by lighter greyscale colour. Red circles show subsample locations for U-Th dating and black squares show areas for thin sections.

U-Th dating

Eight subsamples of BR1, BR2 and BR3 were drilled along the growth layers near their top and bottom for U-Th series dating (Table 1; Fig. 3). Replication tests were performed on each subsample. U and Th were then separated and purified following the chemical procedure described in Edwards *et al.* (1986). U-Th isotopic measurement was performed on a Thermo Finnigan Neptune Plus multi-collector inductively coupled plasma mass spectrometer (MC-ICP-MS) in the isotope geochemistry laboratory at the Earth Observatory of Singapore, Nanyang Technological University, Singapore. The U and Th isotopes were measured on a secondary electron multiplier using peak jumping mode (Shen *et al.* 2012; Cheng *et al.* 2013).

Table 1 U and Th isotopic compositions (238 U, 234 U, 232 Th, and 230 Th) and U-Th ages for subsamples of stalagmites BR1, BR2 and BR3. U decay constants: $\lambda_{238} = 1.55125 \times 10^{-10}$ (Jaffey *et al.* 1971) and $\lambda_{234} = 2.82206 \times 10^{-6}$ (Cheng *et al.* 2013). Th decay constant: $\lambda_{230} = 9.1705 \times 10^{-6}$ (Cheng *et al.* 2013). * δ^{234} U = ($[^{234}$ U/ 238 U] activity – 1) x 1000. ** δ^{234} U_{initial} was calculated based on 230 Th age (T), i.e. δ^{234} U_{initial} = δ^{234} U_{measured} x e $^{\lambda 234}$ XT. Corrected 230 Th ages assume the initial 230 Th/ 232 Th atomic ratio of $4.4\pm2.2 \times 10^{-6}$. Those are the values for a material at secular equilibrium with the bulk earth 232 Th/ 238 U value of 3.8. The errors are arbitrarily assumed to be 50%.

Sample	Number	²³⁸ U (ppb)	²³² T (pp		²³⁰ Th / (atomic		d ²³⁴ l (measi	- 4.		/ ²³⁸ U ivity)	²³⁰ Th a (uncorre		(age, con			Initial** ected)	²³⁰ Th (age, corr	
BR1 top	7A	78	30 562	±615	30	±1	132.7	±2.1	0.7102	±0.0023	104 684	±653	94 528	±7248	173	±4.4	94 464	±7248
BR1 top	7B	75	31 410	±631	27	±1	138.5	±2.1	0.6862	±0.0032	98 152	±798	87 343	±7728	177	±4.7	87 278	±7728
BR1 bottom	8A	44	2806	±57	172	±4	143.7	±2.0	0.6575	±0.0032	91 115	±729	89 553	±1317	185	±2.7	89 488	±1317
BR1 bottom	8B	40	1575	±32	273	±6	146.7	±1.9	0.6566	± 0.0030	90 511	±690	89 534	±971	189	±2.6	89 470	±971
BR 2 top	5A	84	26 950	±541	35	±1	144.4	±2.1	0.6777	±0.0029	95 378	±711	87 227	±5826	185	±4.0	84 162	±5826
BR 2 top	5B	75	9403	±189	87	±2	149.7	±2.1	0.6617	± 0.0026	91 172	±618	88 052	±2289	192	±2.9	87 978	±2289
BR 2 bottom	6A	89	7334	±148	131	±3	145.3	±2.1	0.6576	±0.0023	90 917	±567	88 868	±1552	187	±2.8	88 803	±1552
BR 2 bottom	6B	89	6498	±130	149	±3	146.5	±1.6	0.6576	± 0.0021	90 748	±500	88 951	±1363	188	±2.2	88 887	±1363
BR3 Top big	1A	181	21 239	±428	106	±2	177.6	±2.1	0.7560	±0.0027	108 039	±732	105 253	±2096	239	±3.0	105 118	±2096
BR3 Top big	1B	180	10 042	±202	200	±4	179.9	±2.1	0.6791	±0.0023	90 822	±548	89 494	±1084	232	±3.0	89 429	±1084
BR3 Top small	2A	119	39 624	±797	36	±1	144.7	±2.1	0.7263	±0.0032	106 550	±859	98 117	±6042	191	±4.0	98 052	±6042
BR3 Top small	2B	116	29 348	±590	47	±1	157.3	±2.0	0.7146	±0.0028	101 698	±716	95 434	±4493	206	±4.0	95 369	±4493
BR 3 bottom small	3A	85	32 394	±650	31	±1	157.8	±2.0	0.7228	±0.0028	103 518	±720	93 990	±6809	206	±4.7	93 925	±6809
BR 3 bottom small	3B	82	12 161	±244	78	±2	155.4	±2.0	0.7017	±0.0023	99 080	±596	95 443	±2639	203	±3.1	95 378	±2639
BR 3 bottom big	4A	48	10 654	±214	53	±1	164.3	±1.9	0.7216	±0.0028	102 216	±716	96 731	±3948	216	±3.5	96 666	±3948
BR 3 bottom big	4B	47	9754	±196	56	±1	161.2	±2.1	0.7148	±0.0028	101 154	±727	96 025	±3700	211	±3.6	95 960	±3700

3. Results and discussion

Physical properties and CT images

Sample BR1 has a nearly symmetrical candle shape with a length of 31 cm and a diameter between 6 and 8 cm. The colour is yellowish grey. The rough outer surface shows some visible macro-holes (Fig. 2A). Along the axis, the halved samples display small cavities and discontinuities. The growth axis clearly shifted with time as the drip point moved laterally, giving rise to an asymmetric stalagmite so that only one flank of the underlying edifice was partially coated (Fig. 3).

Sample BR2 is approximately 28 cm in height and ranges from 8 cm to 10 cm in diameter. The shape is a nearly symmetrical candle with a larger diameter in the middle part. Compared to BR1, the yellowish grey BR2 exhibits darker colours on its weathered outer surface. The surface texture is irregular, rough and has some visible macro-holes at the bottom (Fig. 2A). The cut sample shows growth layers with darker bands interlayered with lighter bands. There are several obvious discontinuities (hiatus; Fig. 3).

Sample BR3 is significantly different from BR1 and BR2 in shape. It incorporates a smaller stalagmite in its lower portion. The length of the outer stalagmite is 36 cm and the diameter 8-11 cm. The inner stalagmite has a length of 26 cm and a diameter of 3-6 cm. Both stalagmites have an asymmetric shape with the smallest diameter in their middle. Growth layers and growth axis of the inner stalagmite are unlike the outer one (Fig. 3). The boundary between the stalagmites is characterized by a discontinuity. The porosity is high on the flanks of the two stalagmites.

In Fig. 3, CT images are displayed in greyscale. Lighter greyscale values indicate higher densities. Lower densities are observed in areas with high porosity or a hiatus (Fig. 3). The cut samples of BR1 and BR3 show axis holes (diameter >1 mm) extending parallel to the growth axis (Fig. 4). The axis holes were also previously observed in CT scan images of uncut samples (Fig. 3). This feature can be caused by an elongated dissolution process that affects the primary porosity of columnar calcite and is initiated particularly as elongated cavities along the boundaries between neighbouring crystals (Perrin *et al.* 2014). The dissolution process gradually enlarges secondary voids. Their width varies from a few micrometres to a few hundreds of micrometres. In the last stage, these dissolution cavities become connected to each other and form a framework of micro-holes in the central part of the stalagmite (Perrin

et al. 2014). The cut sample of BR2 shows its central voids with depression downward across the layers (Fig. 4), where the CT image indicates lower densities. This feature may be caused by under-saturated or corrosive water cutting through the growth layers along micro-fractures inside as off-axis holes (Shtober-Zisu et al. 2014).

The internal dissolution feature and shift of growth axis suggest that the samples BR1, BR2 and BR3 have suffered significant depositional changes during or after their growths. These changes however cannot be readily predicted from the uncut stalagmites. The CT images conversely reveal that the samples have significant density variations and contain small and large voids (Fig. 3). Obviously, the CT images provide unique information about the internal structure of stalagmites that cannot be identified by visual inspection of the uncut specimens (Fig. 2B, 3).

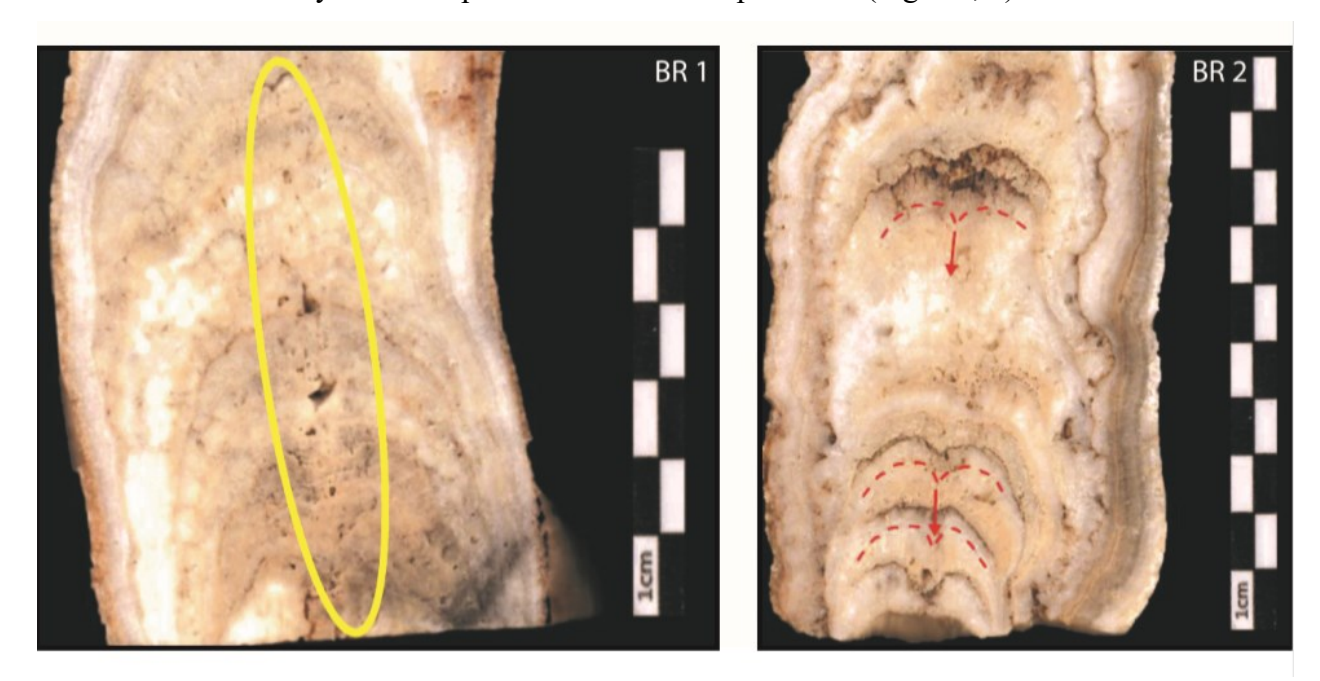


Fig. 4. Samples BR1 and BR2 showing axis holes elongated parallel to the growth axis with diameter ranging from 1 to 5 mm. In BR2, the marked feature shows downward bending of growth layers towards to the holes.

Petrography and density

Petrographic analysis of polished thin sections can facilitate identifying different types of calcite fabrics in the stalagmites (Frisia 2015). We prepared nineteen polished thin sections from samples BR1, BR2 and BR3. Four fabric types can be observed (Fig. 5A-H, see positions of polished thin sections in Fig. 3): (i) Open Dendritic fabric

formed interlocking and elongated crystals with spatial distribution. This texture is characterized by high porosity (Frisia *et al.* 2000, 2002). (ii) Closed dendritic fabric has more equal dimensions and forms less porous lamina. (iii) Columnar fabric is characterized by large crystals growing parallel to the central axis. Their crystal boundaries are acute. In general, the columnar fabric is less porous than the dendritic fabric (Frisia 2015). (iv) Micritic layers are observed mainly on the edges of the stalagmite BR3.

In this study, variations in the crystalline fabric as well as the porosities are represented in the CT numbers (HU) in Table 2. The open dendritic fabric shows a high porosity with the lowest density (<1200 HU). Closed dendritic has a medium density (1200-1400 HU). Columnar fabric has the highest density (1401-1550 HU). The calcite fabrics and CT numbers (HU) of Tham Nam stalagmites were then compared to those previously reported in Vanghi et al. (2015), Walczak et al. (2015) and Frisia (2015) (Table 2). Stalagmites BR1, BR2 and BR3 display CT numbers (HU) <1550, and fabrics indicate variable drip rates and fast growth rates (Frisia 2015). Density in a speleothem is related to primary crystalline texture and porosity. Secondary porosity can be the result of dissolution and/or fractures that lead to lower density. Diagenesis can cause loss of primary texture, mineralogy and geochemical signatures (Perrin et al. 2014; Scholz et al. 2014; Zhang et al. 2014; Bajo et al. 2016). Thus, the present work, in agreement with previous studies (Vanghi et al. 2015; Walczak et al. 2015), suggests that the areas within stalagmites regarded suitable for palaeoclimatic study, should exhibit primary crystalline texture, low porosity and CT numbers (HU) of 1550 or higher.

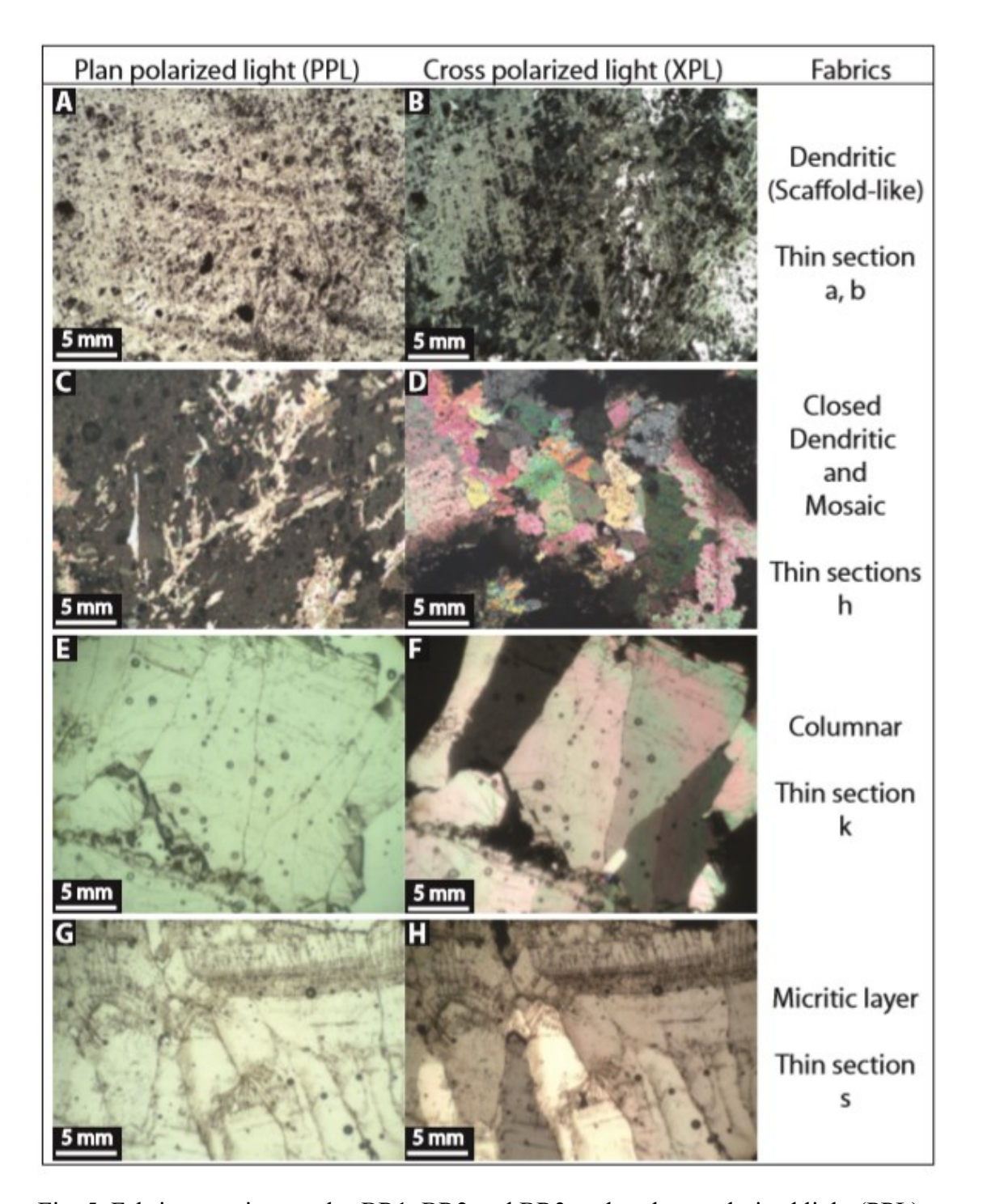


Fig. 5. Fabric types in samples BR1, BR2 and BR3 under plane polarized light (PPL) and cross-polarized light (XPL).

U-Th dating

All U-Th ages of the subsamples from stalagmites BR1, BR2 and BR3 are replicable within uncertainties, except for 1A and 1B (Table 1; Fig. 3). In fact, in each pair of replicates, the difference between the mean ages is much smaller than the uncertainty (2 σ), which suggests that the U-Th chemical separations and machine measurements are robust. The measured ²³⁸U concentrations and δ^{234} U values can also be well replicated. However, the ²³²Th content and values of ²³⁰Th/²³²Th atomic ratio show considerable variation. This Th heterogeneity is probably due to an uneven distribution of detritus, which contains high Th contents. The discrepancy in U-Th ages between subsamples 1A and 1B near the top layer of stalagmite BR3 is likely caused by a diagenetic process (e.g., dissolution, recrystallization and neomorphism) because they were drilled in the low-density part of the sample (Fig. 3).

²³⁸U concentrations in all the samples are lower than 200 ppb and ²³²Th concentrations range from thousands to tens of thousands of ppt. The isotopic ratios of ²³⁰Th to ²³²Th are also low, typically less than 200 ppm. This unfortunately limits the age precisions, which largely depend on the ²³⁰Th initial correction. A low ²³⁸U concentration and particularly low ²³⁰Th/²³²Th values indicate that a significant portion of ²³⁰Th does not originate from in situ decay of ²³⁸U. The large uncertainty of the detrital ²³⁰Th/²³²Th in bulk earth values thus dominates the age uncertainties. Nevertheless, if the ²³²Th concentration in the subsample is low and the measured ²³⁰Th/²³²Th value is high, the relative uncertainty of the corrected age can easily be reduced to ~1% or better (e.g., BR1 bottom (8B), Table 1). After the initial Th correction, all the U-Th ages of BR1, BR2 and BR3 are concentrated in a small interval, ranging between 87 and 105 ka. This confirms that they were deposited during the same time interval.

CT images, petrography and U-Th isotope data indicate the dissolution features in the internal structure of stalagmites BR1, BR2 and BR3. This can be caused by several scenarios, for example, (i) undersaturated or acidic dripping water with high content of pCO₂ (Perrin *et al.* 2014), (ii) abruptly increasing dripping water rate, which prevents sufficient degassing to bring feeding water to equilibrium with CaCO₃ (Railsback *et al.* 2011) or (iii) mixing dissolution solution with several drip water sources (Scholz *et al.* 2014). Recent studies suggest that microbial activity can affect calcification through trapping and binding detrital particles and inducing calcite precipitation. This leads to breakdown dissolution, boring and residue micrite

production (Jones 2001; Shtober-Zisu *et al.* 2014). Such processes can change the primary isotopic and elemental composition of a speleothem. These changes alter the geochemical signals, which may have an impact on the interpretation of the results obtained in palaeoenvironmental studies (Martín-García *et al.* 2009). Typically, stalagmite samples containing these features are no longer suitable for palaeoclimate studies. For speleothem age determination, carbonate samples must have remained completely closed with respect to loss or gain of U and Th isotopes. For example, Bajo *et al.* (2016) reported that U-Th ages could be overestimated in a stalagmite that has anomalously high ²³⁰Th/²³⁸U isotopic ratios resulting from preferentially U loss in in micro-void dissolution. Based on CT images, petrography analysis and large uncertainty of ²³⁰Th/²³²Th, we hereby decided not to perform any additional dating and geochemical analysis on the stalagmites from Tham Nam cave.

Table 2. Characteristics of CT number (HU values), petrography, and palaeoenvironment of stalagmites.

This	This study		al. (2015)	Walczak et al. (2015) and Frisia (2015)						
HU values	Fabrics	HU values	Fabrics	HU values	Fabrics	Growth rate	Drip rate			
<1200	Opened dendritic	<226	Porous	<2000	Columnar microcrystalline, Dendritic	Fast	Not stable and seasonally variable			
		227-776	Dendritic							
1200-1400	Closed dendritic	77-1176	Closed dendritic							
1401-1550	Columnar	1177-1576	Columnar							
		1577-3071	Micrite	2000- 2400	Opened columnar	Medium	Constant with high drip rate			
				>2400	Compacted columnar	Slow	Constant with low drip rate			

4. Conclusions

In the present work, stalagmites from Tham Nam cave, western Thailand are evaluated for their palaeoclimatic research potential, through X-ray computed tomography (CT scanning), petrography, and U-Th dating analysis. The CT scanning data reveal that stalagmite density is associated with fabrics and distribution of porosity. The porosity/axis-holes/voids in the stalagmites are related to postdepositional dissolution processes and may have an influence on U-Th dating accuracy. The ages of stalagmites from the Tham Nam Cave range between 87 and 105 ka. Currently, they are the oldest stalagmites that have been reported from mainland Southeast Asia. However, the stalagmites show dissolution features, several discontinuities and large age uncertainty, so that they are likely not suitable for palaeoclimatic research. Consistent with previous work (Mickler et al. 2004; Zisu et al. 2012; Vanghi et al. 2015; Walczak et al. 2015 and Bajo et al. 2016), this study suggests that CT images have a large yet underestimated potential in speleothem study. It can help to identify internal structures in samples that may compromise geochemical elemental and isotopic analyses. For stalagmites, potentially suitable for palaeoenvironmental research, CT-scanning can also facilitate selection of the right cutting location. This study hence sets an example for future speleothem exploration using CT scanning as a tool to examine petrological textures prior to any further analysis.

5. Recommendation for future work

Given the lack of paleo-precipitation records from Southeast Asia, it is important to examine whether stalagmites record from Thailand can be added as an archive of tropical climate change or whether the environmental signals stored in the cave are recorders of local impact.

A valid reconstruction of the temporal and spatial variability of past monsoon precipitation patterns and a better understanding of the underlying causes need more high-resolution hydroclimatic records from the Asian monsoon region. Only such a dense network of well-dated, multi-proxy data sets will allow reducing the current uncertainties and will provide a valid base for discussing the response of different proxies used to infer hydroclimatic conditions and leads and lags in response to past rainfall intensities.

6. References

Bajo, P., Hellstrom, J., Frisia, S., Drysdale, R., Black, J., Woodhead, J., Borsato, A., Zanchetta, G., Wallace, M. W., Regattieri, E. & Haese, F. 2016: "Cryptic" diagenesis and its implications for speleothem geochronologies. Quaternary Science Reviews 148, 17-28.

Cai, B., Pumijumnong, N., Tan, M., Muangsong, C., Kong, X., Jiang, X. & Nan, S. 2010: Effects of intraseasonal variation of summer monsoon rainfall on stable isotope and growth rate of a stalagmite from northwestern Thailand. Journal of Geophysical Research: Atmospheres 115, D21104.

Cai, Y., Fung, I. Y., Edwards, R. L., An, Z., Cheng, H., Lee, J. E., Tan, L., Shen, C.C., Wang, X., Day, J. A., Zhou, W., Kelly, W. & Chiang, J. 2015: Variability of Stalagmite-Inferred Indian Monsoon Precipitation over the Past 252,000 Y. Proceedings of the National Academy of Sciences 112, 2954–2959.

Chen, F., Xu, Q., Chen, J., Birks, H. J. B., Liu, J., Zhang, S., Jin, L., An, C., Telford, R. J., Cao, X., Wang, Z., Zhang, X., Selvaraj, K., Lu, H., Li, Y., Zheng, Z., Wang, H., Zhou, A., Dong, G., Zhang, J., Huang, X., Bloemendal, J. & Rao, Z. 2015: East Asian summer monsoon precipitation variability since the last deglaciation. Scientific Reports 5, 11186.

Cheng, H., Edwards, R. L., Shen, C. C., Polyak, V. J., Asmerom, Y., Woodhead, J., Hellstrom, J., Wang, Y., Kong, X., Spötl, C., Wang, X. & Calvin Alexander Jr., E. 2013: Improvements in 230Th dating, 230Th and 234U half-life values, and U–Th isotopic measurements by multi-collector inductively coupled plasma mass spectrometry. Earth and Planetary Science Letters 371, 82–91.

Cook, E. R., Anchukaitis, K. J, Buckley, B. M., D'Arrigo, R.D., Jacoby, G. C. & Wright, W. E. 2010: Asian Monsoon Failure and Megadrought During the Last Millennium. Science 328, 486–89.

Department of Mineral Resources (DMR). 2009: Geological Map of Thailand

- (Uthai Thani) Scale 1: 250000, Ministry of natural resource and environment, Bangkok, Thailand.
- Edwards, R. L., Chen, J. H. & Wasserburg, G. J. 1986: 238U-234U-230Th-232Th systematics and the precise measurement of time over the past 500,000 years. Earth and Planetary Science Letters 81, 175–192.
- Fairchild, I. J., Smith, C. L., Baker, A., Fuller, L., Spötl, C., Mattey, D. & McDermott, F. 2006: Modification and preservation of environmental signals in speleothems. Earth-Science Reviews 75, 105–153.
- Fairchild, I. J, Frisia, S., Borsato, A. & Tooth, A. F. 2007: Speleothems. in Geochemical Sediments and Landscapes (eds D. J. Nash and S. J. McLaren), 200-245, Blackwell Publishing Ltd, Oxford, UK.
- Fairchild, I. J.& Treble, P. C. 2009: Trace elements in speleothems as recorders of environmental change. Quaternary Science Reviews 28, 449–468.
- Frisia, S. 2015: Microstratigraphic logging of calcite fabrics in speleothems as tool for palaeoclimate studies. International Journal of Speleology 44, 1-16.
- Frisia, S., Borsato, A., Fairchild, I. J. & McDermott, F. 2000: Calcite Fabrics, Growth Mechanisms, and Environments of Formation in Speleothems from the Italian Alps and Southwestern Ireland. Journal of Sedimentary Research 70, 1183–1196.
- Frisia, S., Borsato, A., Fairchild, I. J., McDermott, F. & Selmo, E. M. 2002: Aragonite-calcite relationships in speleothems (Grotte de Clamouse, France): Environment, fabrics, and carbonate geochemistry. Journal of Sedimentary Research 72, 687–699.
- Hendy, C. H. 1971: The isotopic geochemistry of speleothems—I. The calculation of the effects of different modes of formation on the isotopic composition of speleothems and their applicability as palaeoclimatic indicators. Geochimica et Cosmochimica Acta 35, 801–24.
- Jaffey, A. H., Flynn, K. F., Glendenin, L. E., Bentley, W. T. & Essling, A. M. 1971: Precision measurement of half-lives and specific activities of 235U and 238U. Physical Review C4, 1889.
- Jones, B. 2001: Microbial Activity in Caves A Geological Perspective. Geomicrobiology Journal 18, 345–357.
- Ketcham, R. A., & Carlson, W. D. 2001: Acquisition, optimization and interpretation of X-ray computed tomographic imagery: applications to the geosciences. Computers & Geosciences 27, 381-400.
- Lachniet, M. S. 2009: Climatic and environmental controls on speleothem oxygen-isotope values. Quaternary Science Reviews 28, 412–432.
- Loo, Y. Y., Billa, L. & Singh, A. 2015: Effect of climate change on seasonal monsoon in Asia and its impact on the variability of monsoon rainfall in Southeast Asia. Geoscience Frontiers 6, 817-823.
- Martín-García, R., Alonso-Zarza, A. M. & Martín-Pérez, A. 2009: Loss of primary texture and geochemical signatures in speleothems due to diagenesis: evidences from Castañar Cave, Spain. Sedimentary Geology 221, 141-149.
- McDermott, F. 2004: Palaeo-climate reconstruction from stable isotope variations in speleothems: a review. Quaternary Science Reviews 23, 901–918.
- Mickler, P. J., Ketcham, R. A., Colbert, M. W. & Banner, J. L. 2004: Application of high-resolution X-ray computed tomography in determining the suitability of speleothems for use in palaeoclimatic, palaeohydrologic reconstructions. Journal of Cave and Karst Studies 66, 3–8.
- Mickler, P. J., Banner, J. L., Stern, L., Asmerom, Y., Edwards, R. L., & Ito, E. 2004: Stable isotope variations in modern tropical speleothems: evaluating equilibrium vs. kinetic isotope effects. Geochimica et Cosmochimica Acta 68, 4381–

4393.

Muangsong, C., Cai, B., Pumijumnong, N., Hu, C. & Cheng, H. 2014: An annually laminated stalagmite record of the changes in Thailand monsoon rainfall over the past 387 years and its relationship to IOD and ENSO. Quaternary International 349, 90–97.

Muangsong, C., Cai, B., Pumijumnong, N., Hu, C. & Lei, G. 2016: Intra-seasonal variability of teak tree-ring cellulose δ18O from northwestern Thailand: A potential proxy of Thailand summer monsoon rainfall. The Holocene 26, 1397–1405.

Perrin, C., Prestimonaco, L., Servelle, G., Tilhac, R., Maury, M. & Cabrol, P. 2014: Aragonite–calcite speleothems: identifying original and diagenetic features. Journal of Sedimentary Research 84, 245–269.

Raghavan, S. V., Liu, J., Nguyen, N. S., Vu, M. T. & Liong, S. Y. 2017: Assessment of CMIP5 historical simulations of rainfall over Southeast Asia. Theoretical and Applied Climatology, 1–14.

Railsback, L. B., Dabous, A. A., Osmond, J. K. & Fleisher, C. J. 2002: Petrographic and geochemical screening of speleothems for U-series dating: an example from recrystallized speleothems from Wadi Sannur Cavern, Egypt. Journal of Cave and Karst Studies 64, 108-116.

Railsback, L. B., Liang, F., Romaní, J. R. V., Grandal-d'Anglade, A., Rodríguez, M. V., Fidalgo, L. S., Mosquera, D. F., Cheng, H. & Edwards, R. L. 2011: Petrographic and isotopic evidence for Holocene long-term climate change and shorter-term environmental shifts from a stalagmite from the Serra do Courel of northwestern Spain, and implications for climatic history across Europe and the Mediterranean. Palaeogeography, Palaeoclimatology, Palaeoecology 305, 172–184.

Scholz, D., Tolzmann, J., Hoffmann, D. L., Jochum, K. P., Spötl, C. & Riechelmann, D. F. 2014: Diagenesis of speleothems and its effect on the accuracy of 230Th/U-ages. Chemical Geology 387, 74–86.

Shen, C. C., Wu, C. C., Cheng, H., Edwards, R. L., Hsieh, Y. T., Gallet, S., Chang, C.-C., Li, T.-Y., Lam, D. D., Kano, A., Hori, M. & Spötl, C. 2012: High-precision and high-resolution carbonate 230Th dating by MC-ICP-MS with SEM protocols. Geochimica et Cosmochimica Acta 99, 71–86.

Shtober-Zisu, N., Schwarcz, H. P., Chow, T., Omelon, C. R. & Southam, G. 2014: Caves in caves: evolution of post-depositional macroholes in stalagmites. International Journal of Speleology 43, 323-334.

Sinha, A., Kathayat, G., Cheng, H., Breitenbach, S. F., Berkelhammer, M., Mudelsee, M., Biswas, J. & Edwards, R. L. 2015: Trends and Oscillations in the Indian Summer Monsoon Rainfall over the Last Two Millennia. Nature Communications 6, ncomms7309.

Sinha, A., Stott, L., Berkelhammer, M., Cheng, H., Edwards, R. L., Buckley, B., Aldenderfer, M. & Mudelsee, M. 2011: A global context for megadroughts in monsoon Asia during the past millennium. Quaternary Science Reviews 30, 47–62.

Thirumalai, K., DiNezio, P.N, Okumura, Y. & Deser, C. 2017: Extreme temperatures in Southeast Asia caused by El Niño and worsened by global warming. Nature Communications 8, ncomms15531.

Vanghi, V., Iriarte, E. & Aranburu, A. 2015: High resolution X-ray computed tomography for petrological characterization of speleothems. Journal of Cave and Karst Studies 77, 75–82.

Walczak, I. W., Baldini, J. U., Baldini, L. M., McDermott, F., Marsden, S., Standish, C. D., Richards, D.A., Andreo, B. & Slater, J. 2015: Reconstructing high-resolution climate using CT scanning of unsectioned stalagmites: A case study identifying the mid-Holocene onset of the Mediterranean climate in southern Iberia.

Quaternary Science Reviews 127, 117–128.

Wong, C. I. & Breecker, D. O. 2015: Advancements in the use of speleothems as climate archives. Quaternary Science Reviews 127, 1–18.

Zhang, P., Cheng, H., Edwards, R. L., Chen, F., Wang, Y., Yang, X., Liu, J. An, C., Dai, Z., Zhou, J., Zhang, D., Jia, J., Jin, L. & Johnson, R. K. 2008: A test of climate, sun, and culture relationships from an 1810-year Chinese cave record. Science 322, 940–942.

Zhang, H., Cai, Y., Tan, L., Qin, S. & An, Z. 2014: Stable isotope composition alteration produced by the aragonite-to-calcite transformation in speleothems and implications for palaeoclimate reconstructions. Sedimentary Geology, 309, 1-14.

Zisu, N. S., Schwarcz, H. P, Konyer, N., Chow, T. & Noseworthy, M. D. 2012: Macroholes in stalagmites and the search for lost water. Journal of Geophysical Research: Earth Surface 117, F03020.

7. Researchers and affiliations

Sakonvan Chawchai^{1*}, Guangxin Liu², Raphael Bissen³, Kampanart Jankham¹, Warisa Paisonjumlongsri¹, Pitsanupong Kanjanapayont¹, Vichai Chutakositkanon¹, Montri Choowong¹, Santi Pailoplee¹, Xianfeng Wang²

¹MESA Research Unit, Department of Geology, Faculty of Science, Chulalongkorn University, Bangkok, Thailand

²Earth Observatory of Singapore and Asian School of the Environment, Nanyang Technological University, Singapore

³Department of Mining and Petroleum Engineering, Faculty of Engineering, Chulalongkorn University, Bangkok, Thailand.

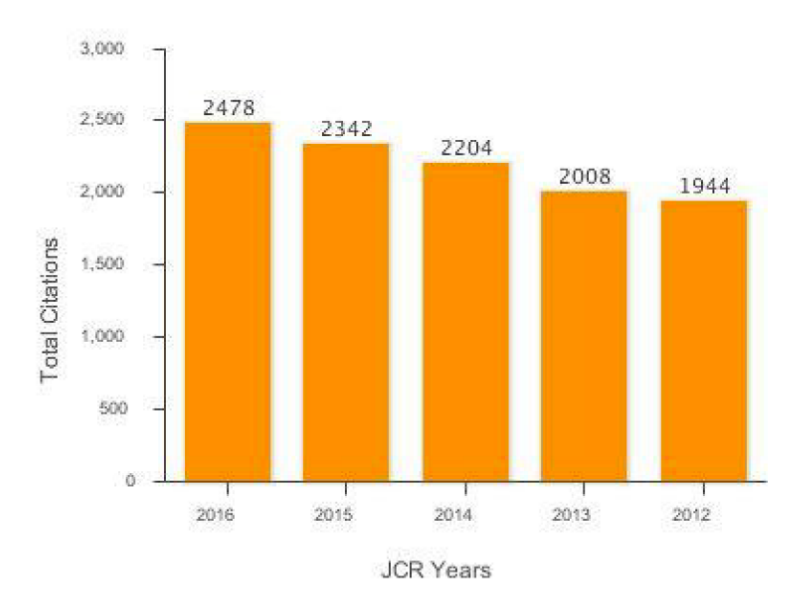
1. ผลงานตีพิมพ์ในวารสารวิชาการนานาชาติ

Sakonvan Chawchai, Guangxin Liu, Raphael Bissen, Kampanart Jankham, Warisa Paisonjumlongsri, Pitsanupong Kanjanapayont, Vichai Chutakositkanon, Montri Choowong, Santi Pailoplee, Xianfeng Wang. "Stalagmites from western Thailand: preliminary investigations and challenges for palaeoenvironmental research", Boreas 47(1), 2018, 367-376 (Impact Factor (2016) 2.348) (อยู่ในฐานข้อมูล ISI)



Journal Profile: BOREAS

Essential Science Indicators : Total Citations Graph



Journal Citation Report : Impact factor

JCR Year	GEOGRAPHY, PHY	/SICAL		GEOSCIENCES, M	ULTIDISCIPLINARY		GEOSCIENCES, INTERDISCIPLINARY			
och fear	Rank	Quartile	JIF Percentile	Rank	Quartile	JIF Percentile	Rank	Quartile	JIF Percentile	
2016	26/49	Q3	47.959	67/188	Q2	64.628	NA	NA	NA	
2015	18/49	Q2	64.286	49/184	Q2	73.641	NA	NA	NA	
2014	16/46	Q2	66.304	39/175	Q1	78.000	NA	NA	NA	
2013	21/46	Q2	55.435	50/174	Q2	71.552	NA	NA	NA	
2012	18/45	Q2	61.111	44/172	Q2	74.709	NA	NA	NA	
2011	18/44	Q2	60.227	54/170	Q2	68.529	NA	NA	NA	
2010	7/42	Q1	84.524	19/167	Q1	88.922	NA	NA	NA	
2009	6/36	Q1	84.722	20/155	Q1	87.419	NA	NA	NA	
2008	11/31	Q2	66.129	31/144	Q1	78.819	NA	NA	NA	
2007	9/31	Q2	72.581	32/137	Q1	77.007	NA	NA	NA	
2006	10/31	Q2	69.355	33/131	Q2	75.191	NA	NA	NA	
2005	NA	NA	NA	11/129	Q1	91.860	NA	NA	NA	
2004	NA	NA	NA	28/128	Q1	78.516	NA	NA	NA	
2003	NA	NA	NA	43/128	Q2	66.797	NA	NA	NA	
2002	NA	NA	NA	41/122	Q2	66.803	NA	NA	NA	
2001	NA	NA	NA	7/117	Q1	94.444	NA	NA	NA	
2000	NA	NA	NA	NA	NA	NA	22/117	Q1	81.624	

Copyright © 2017 Clarivate Analytics

By exporting the selected data, you agree to the data usage policy set forth in the Terms of Use

Stalagmites from western Thailand: preliminary investigations and challenges for palaeoenvironmental research

SAKONVAN CHAWCHAI D, GUANGXIN LIU, RAPHAEL BISSEN, KAMPANART JANKHAM, WARISA PAISONJUMLONGSRI, PITSANUPONG KANJANAPAYONT, VICHAI CHUTAKOSITKANON, MONTRI CHOOWONG, SANTI PAILOPLEE AND XIANFENG WANG

BOREAS



Chawchai, S., Liu, G., Bissen, R., Jankham, K., Paisonjumlongsri, W., Kanjanapayont, P., Chutakositkanon, V., Choowong, M., Pailoplee, S. & Wang, X. 2018 (January): Stalagmites from western Thailand: preliminary investigations and challenges for palaeoenvironmental research. *Boreas*, Vol. 47, pp. 367–376. https://doi.org/10.111/bor.12299. ISSN 0300-9483.

Locating suitable caves and stalagmites for palaeoenvironmental and palaeoclimatic studies can be challenging. Isotopic geochemical analyses, albeit commonly performed for palaeoclimatic reconstruction, are also time consuming and costly. Therefore, petrographic and non-destructive morphological studies on speleothems are desirable to facilitate sample selection for further analysis. In this study, 20 caves were surveyed in Ban Rai district, Uthai Thani province in western Thailand. After external physical observations in the field, three stalagmite samples were collected from Tham Nam Cave to test their potential for palaeoclimatic research. Firstly, the stalagmites were scanned by X-ray computed tomography (CT scanning) and subsequently the CT images were compared with petrographic inspections. Columnar fabrics show the highest density, whereas closed and open dendritic fabrics have medium and the lowest densities, respectively. Layers near the top and bottom of the three stalagmites were dated by U-Th mass spectrometric techniques. All three samples were deposited between c. 87 and c. 105 ka ago; therefore, they are probably the oldest stalagmites that have been reported so far from mainland Southeast Asia. However, their physical features indicate that all the samples have suffered from postdepositional dissolution, and are unlikely to be suitable for palaeoclimatic research. The internal dissolution feature of stalagmites, however, cannot be identified by visual inspection of uncut samples. We hereby argue that CT images are useful to characterize stalagmite petrography, in particular fabric, porosity and density. Such features can be used to select the ideal plane of a stalagmite for sectioning, to maximize the chances of robust climatic reconstruction.

Sakonvan Chawchai (sakonvan.c@chula.ac.th), Kampanart Jankham, Warisa Paisonjumlongsri, Pitsanupong Kanjanapayont, Vichai Chutakositkanon, Montri Choowong and Santi Pailoplee, MESA Research Unit, Department of Geology, Faculty of Science, Chulalongkorn University, Bangkok 10330, Thailand; Guangxin Liu and Xianfeng Wang, Earth Observatory of Singapore and Asian School of the Environment Nanyang Technological University, Singapore 639798, Singapore; Raphael Bissen, Department of Mining and Petroleum Engineering, Faculty of Engineering, Chulalongkorn University, Bangkok 10330, Thailand; received 24th August 2017, accepted 15th November 2017.

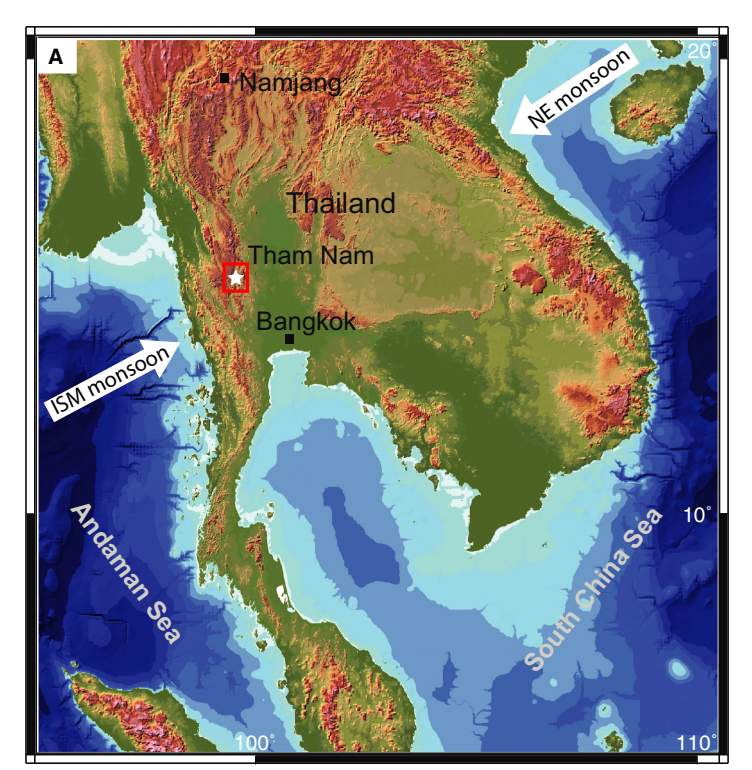
Speleothems are secondary carbonate deposits formed inside caves. Their fabrics, stable isotope ratios, trace element compositions and organic chemistry can record events that occur at the cave surface during their growth history (McDermott 2004; Fairchild et al. 2006). Several types of speleothems (e.g. flowstones, stalactites and stalagmites) have been used as palaeoenvironmental and palaeoclimatic archives to study the changes in local or regional temperature, vegetation and precipitation, thanks to their continuous or semicontinuous deposition, absolute and precise datability, occurrence over a wide range of latitudes and possible conservation of palaeoclimate signals on millennial, decadal and even annual time scales (e.g. Hendy 1971; McDermott 2004; Fairchild et al. 2006; Fairchild & Treble 2009; Lachniet 2009; Mickler et al. 2004a, b; Wong & Breecker 2015). Stalagmites have been favourably used in past hydroclimate reconstruction because of their predominantly columnar shapes and relatively simple sequential depositions (e.g. Zhang et al. 2008; Cai et al. 2010; Chen et al. 2015; Sinha et al. 2015). However, it remains a challenge to find suitable caves and stalagmite samples for palaeoclimatic research because only pristine stalagmites, deposited

under chemical equilibrium conditions, can faithfully record climate signals.

Mainland Southeast Asia (e.g. Thailand, Myanmar, Malaysia peninsula and Laos) is located on the route of moisture transport of the Indian summer monsoon (ISM, Fig. 1A). The agrarian societies dominant in the region heavily rely on the monsoon rainfall. Changes in rainfall intensity and variability therefore have a great impact on people's livelihoods in mainland Southeast Asia (Loo et al. 2015). The projection of future hydroclimatic change in the region demands a good understanding of monsoon rainfall history (Cook et al. 2010; Raghavan et al. 2017; Thirumalai et al. 2017). Instrumental records of precipitation and temperature are however short (<50 years) and sparse in mainland Southeast Asia. Hence, palaeoclimate proxy data have to be applied to delineate the natural variability as well as anthropogenic contribution to climate change. Yet, such studies are still scarce in mainland Southeast Asia.

The beauty of the caves and speleothems in mainland Southeast Asia has attracted millions of tourists and visitors from around the world. Stalagmites from this region however have rarely been investigated for palaeoen-vironmental research. In Thailand for instance, only two

368 Sakonvan Chawchai et al. BOREAS



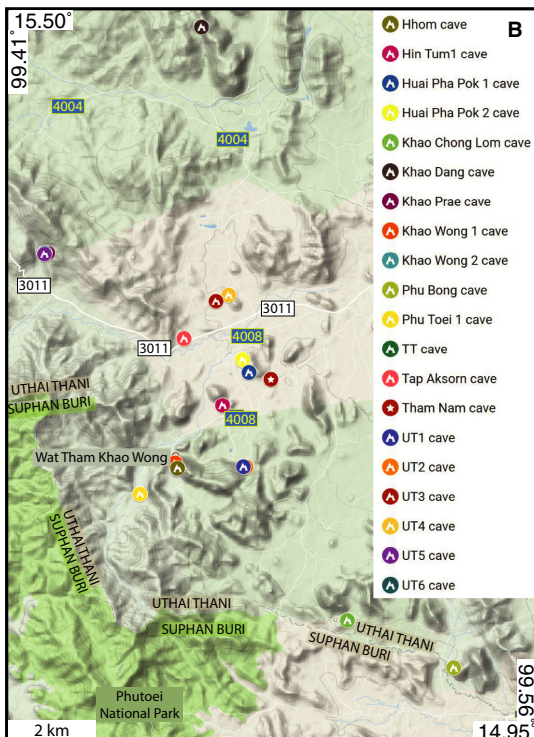


Fig. 1. A. Locations of Ban Rai district (red square) and Tham Nam Cave (white star) in Uthai Thani, western Thailand. B. Locations of the 20 surveyed caves in Ban Rai, Uthai Thani province. [Colour figure can be viewed at www.boreas.dk]

stalagmite records have been reported so far. In these studies, stalagmites from the Namjang Cave, Mae Hong Son province in northwestern Thailand (Fig. 1A), were used to reconstruct monsoon variability covering the last 1700 and 400 years, respectively (Cai *et al.* 2010; Muangsong *et al.* 2014). Stalagmite growth rates during the last century from Namjang have been correlated with meteorological data, showcasing the potential palaeoclimatic proxy of Thailand monsoon rainfall (Muangsong *et al.* 2014).

In recent years, there have been studies on diagenetic alteration (e.g. dissolution, recrystallization and neomorphism) in speleothems. This process results in the chemical properties of samples being altered, meaning that they no longer represent the original depositional conditions (Perrin et al. 2014; Scholz et al. 2014; Zhang et al. 2014; Bajo et al. 2016). The diagenetic alteration of speleothems can be observed through analysing petrography, internal microstratigraphy and trace elements in samples (Frisia et al. 2002; Railsback et al. 2002). These petrographic and non-destructive morphological studies are important to evaluate speleothems before further chemical analysis.

X-ray computed tomography (CT scanning) is a non-destructive technique for visualizing interior features of opaque solid objects by measuring the intensity of X-rays when they pass through the objects. The principle of computed tomography is to acquire multiple sets of views of an object over a range of angular orientations. These

data are used to create two-dimensional images that are called slices (along the scan plane) and then provide a three-dimensional image of a volume by obtaining a series of contiguous slices (Ketcham & Carlson 2001). CT scanning has previously been used in studying speleothem features, including porosity (Mickler *et al.* 2004a, b), macro-holes and postdepositional off axis holes (Zisu *et al.* 2012), and calcite density (Vanghi *et al.* 2015; Walczak *et al.* 2015), as well as in exploring evidence of diagenesis in speleothems (Bajo *et al.* 2016). It has been proposed that CT images of uncut stalagmites can provide essential information on their petrography to evaluate the potential impact on U-Th ages and isotopic geochemical analyses, which cannot be visually identified instead.

The aims of this study were to find stalagmite samples in Ban Rai district, Uthai Thani province, western Thailand (Fig. 1A, B), based on their external physical properties (e.g. shape, colour and texture), and analyse them with respect to their potential for palaeoclimatic research via CT scanning, petrographic studies and U-Th analysis.

Material and methods

Geological setting

The study area is located in national conservation zones of Ban Rai district, Uthai Thani province, western Thailand (Fig. 1A, B). All caves in this area are overlain

by host rock of argillaceous limestone, which is of Ordovician age as indicated by fossil nautilus and crinoids (Department of Mineral Resources (DMR) 2009).

In this study, 20 caves were explored (Fig. 1A, B). Fifteen of them do not contain any stalagmites; three caves contain broken stalagmites that show visible macro-holes and irregular external surfaces; and the other two caves contain both broken and standing stalagmites. Based on their external features (nearly symmetrical, columnar shapes, no obvious corrosions), three standing stalagmite samples (BR1, BR2 and BR3) were collected from Tham Nam Cave, a 300-m-long cave (latitude 15°03′ N, longitude 99°29′ E; altitude 200 m a.s.l; Fig. 1A, B). The stalagmites were retrieved from a large chamber ~200 m from the cave entrance.

Climate in western Thailand is mainly influenced by the ISM, which brings in torrential rains from the Bay of Bengal. Additional precipitation can be contributed by tropical cyclones from the South China Sea in the east during the summer. Mean annual rainfall in Uthai Thani province is about 1770 mm with 105 rain days on average. Mean annual temperature is around 28° C (data from Thai Meteorological Department, AD 1962–2015).

X-ray computed tomography (CT scanning) and petrography

Firstly, the stalagmites BR1, BR2 and BR3 (Fig. 2) were scanned with X-ray computed tomography (CT scanner) at King Chulalongkorn Memorial Hospital, Bangkok, Thailand. The X-ray computed tomography machine (GE Discovery 750 HD) was operated at a tube voltage of 140 kV and a current intensity of 80 mA. The CT scanner was set to a 0.625-mm slice thickness, with a 0.4-mm overlap between slice spacing. Reconstructed images were exported as Digital Imaging and Communications in Medicine (DICOM) files.

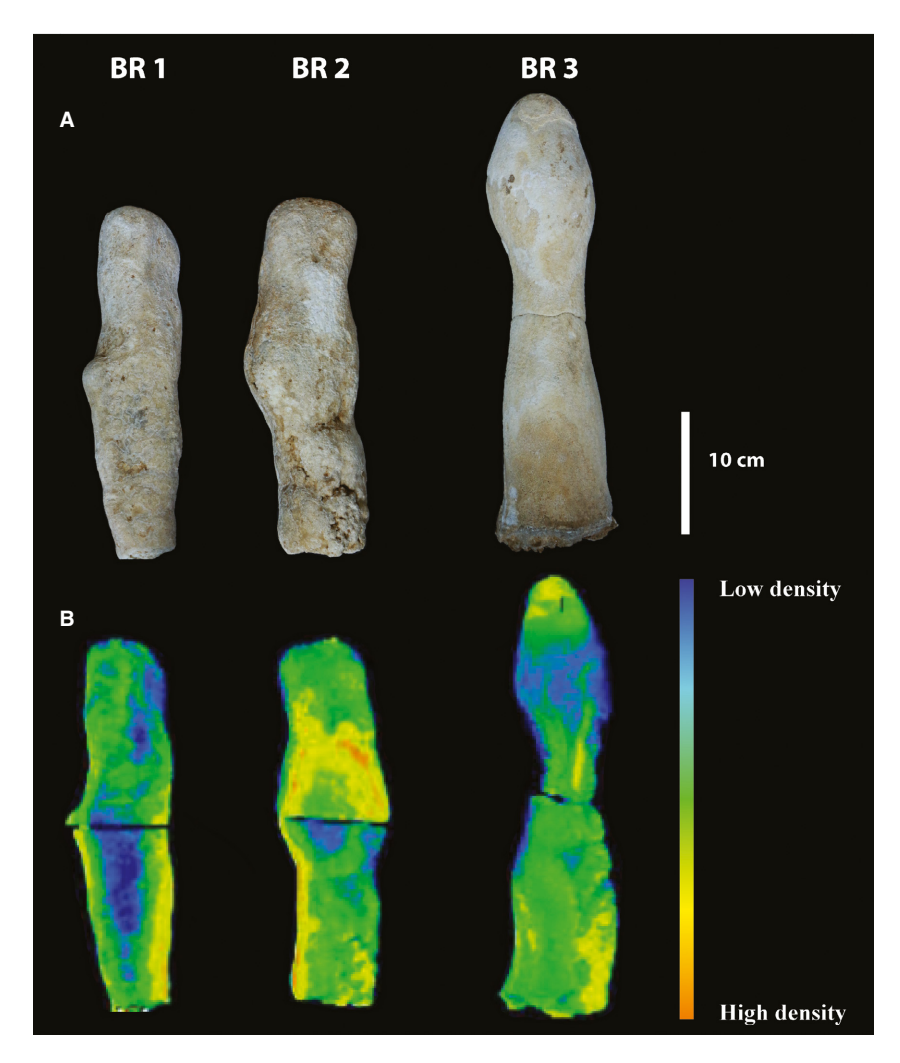


Fig. 2. A. Stalagmite samples BR1, BR2 and BR3. B.2D images of the stalagmites from CT scanning (colour scale: blue colour represents the lowest density; green colour indicates medium density and red/orange colours represent highest density). [Colour figure can be viewed at www.boreas.dk]

When X-rays scan an object, a portion of the radiation can be absorbed or reflected. Such interaction between the X-rays and the object is dependent upon the X-ray energy and the atomic structures of the object. The X-rays that pass through the sample are collected by a detector, which converts them into light radiations. The light radiations are then transformed by a digital camera and later processed by a computer into images (Ketcham & Carlson 2001).

CT numbers in Hounsfield units (HU) define the intensity of the transmitted X-ray beam. The HU is calculated from the relative value of the linear voxel attenuation coefficient (μ voxel) normalized to the reference material water (μ water), which is then multiplied by a magnifying integer constant (Mickler *et al.* 2004a, b): CT numbers in Hounsfield units (HU) = K [(μ voxel- μ water)/ μ water].

CT image processing and data analysis were performed using MeVisLab 2.6.2 software (http://www.mevislab.de/). CT images are shown both in colour (Fig. 2B), and as greyscale images of axial sections (Fig. 3), which indicate the stalagmite's density (Mickler *et al.* 2004a, b; Vanghi *et al.* 2015; Walczak *et al.* 2015); the denser the scanned stalagmites, the brighter the images in CT slices (Fig. 3).

After CT scanning, the plane along the growth axis with less variability in density was chosen for sectioning, and the samples were cut to characterize and describe the different fabrics of the stalagmites. Based on different CT

numbers (HU), 19 polished thin sections were made (Fig. 3).

U-Th dating

Eight subsamples of BR1, BR2 and BR3 were drilled along the growth layers near their top and bottom for U-Th series dating (Table 1; Fig. 3). Replicate tests were performed on each subsample. U and Th were then separated and purified following the chemical procedure described in Edwards *et al.* (1986). U-Th isotopic measurement was performed on a Thermo Finnigan Neptune Plus multi-collector inductively coupled plasma mass spectrometer (MC-ICP-MS) in the isotope geochemistry laboratory at the Earth Observatory of Singapore, Nanyang Technological University, Singapore. The U and Th isotopes were measured on a secondary electron multiplier using peak jumping mode (Shen *et al.* 2012; Cheng *et al.* 2013).

Results and discussion

Physical properties and CT images

Sample BR1 has a nearly symmetrical candle shape with a length of 31 cm and a diameter between 6 and 8 cm. The colour is yellowish grey. The rough outer surface shows some visible macro-holes (Fig. 2A). Along the

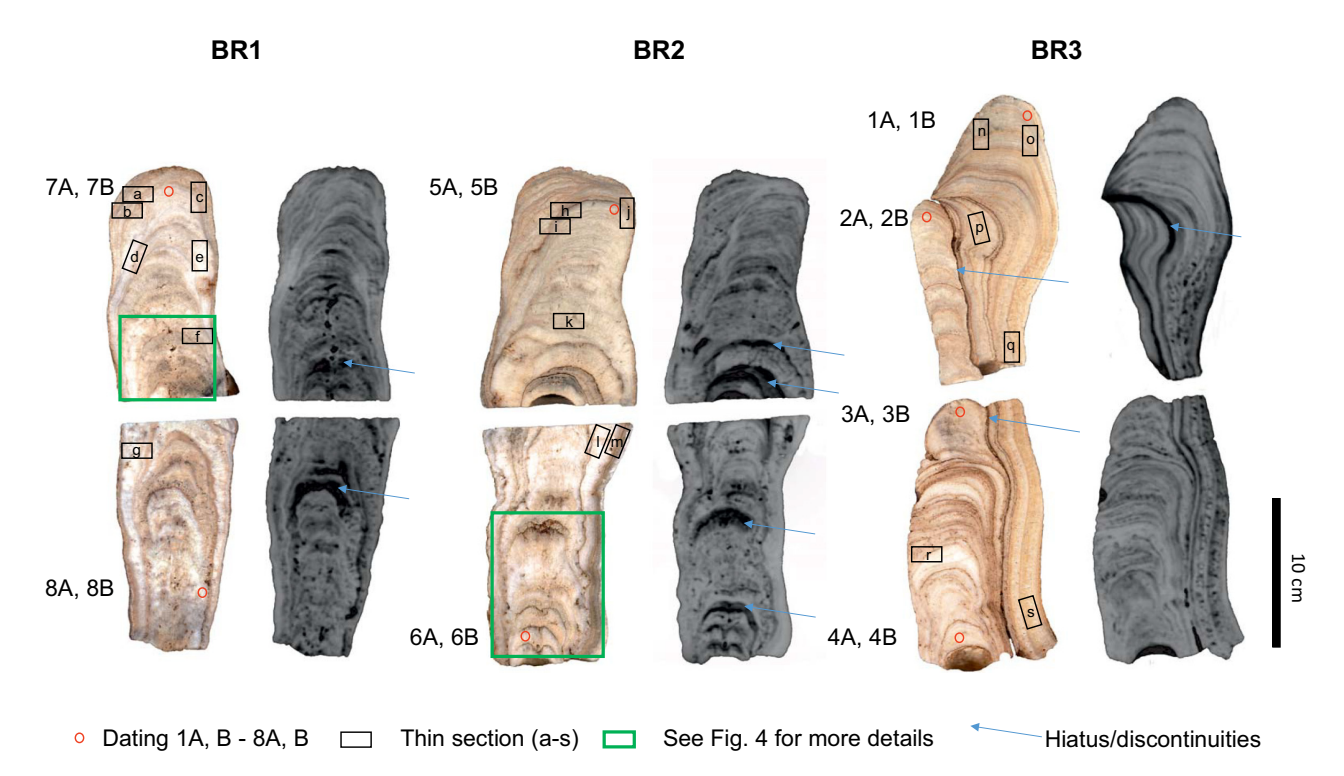


Fig. 3. Halved sections of stalagmites BR1, BR2 and BR3 compared to 2D images of uncut samples from CT scanning in greyscale. Higher densities are indicated by lighter greyscale colour. Red circles show subsample locations for U-Th dating and black rectangles show areas for thin sections. [Colour figure can be viewed at www.boreas.dk]

Table 1. U and Th isotopic compositions (238 U, 234 U, 232 Th and 230 Th) and U-Th ages for subsamples of stalagmites BR1, BR2 and BR3. U decay constants: λ_{238}

and $\lambda_{234} = 2.82206 \times 10^{-6}$ (Cheng et al. 2013). Th decay const (T), i.e. $\delta^{234} U_{\text{inital}} = \delta^{234} U_{\text{measured}} \times e^{\lambda_{234} \times T}$. Corrected $^{23} \text{Th}$ earth $^{232} \text{Th}/^{238} U$ value of 3.8. The errors are arbitrarily assum	10^{-6} (Cheng δ^{234} U $_{\rm measure}$ ie of 3.8. The	Sections ($tet\ al.\ 201$ $d\times e^{\lambda 234\times 1}$ $tet\ errors\ arr$	3). Th decay cons T. Corrected ²³⁰ Th e arbitrarily assur	stant: $\lambda_{230} = 9.1705$ stant: $\lambda_{230} = 9.1705$ and ages assume the immed to be 50%.	in ages for subsatively 3×10^{-6} (Cheng itial 230 Th/ 232 T	imples of stategumes <i>et al.</i> 2013). * δ^{234} U h atomic ratio of 4.4	and h_{13} for the errors are arbitrarily assumed to be 50%. The errors are arbitrarily assumed to be 50%.	uecay constants. λ_{238} -1)×1000. ** δ^{234} Umit ne values for a materia	– 1.35123×10 _{ial} was calculated il at secular equilil	(Jamey et al. 1971) based on ²³⁰ Th age prium with the bulk
Sample	Number	238U (ppb)	²³² Th (ppt)	230 Th/ 232 Th (atomic× 10 =6)	δ^{234} U* (measured)	230 Th/ 238 U (activity)	²³⁰ Th age (years, uncorrected)	²³⁰ Th age (years, corrected)	δ ²³⁴ U _{initial} ** (corrected)	230Th*** age (years, corrected)
BR1 top	7A	78	30 562±615	30±1	132.7 ± 2.1	0.7102 ± 0.0023	104 684±653	94 528±7248	173±4.4	94 464±7248
BR1 top	7B	75	$31\ 410\pm631$	27±1	138.5 ± 2.1	0.6862 ± 0.0032	$98\ 152\pm798$	87 343±7728	177±4.7	87 278±7728
BR1 bottom	8A	4	2806±57	172±4	143.7 ± 2.0	0.6575 ± 0.0032	$91\ 115\pm729$	89 553±1317	185±2.7	89 488±1317
BR1 bottom	8B	40	1575±32	273±6	146.7 ± 1.9	0.6566 ± 0.0030	$90\ 511\pm690$	89 534±971	189 ± 2.6	$89\ 470\pm971$
BR 2 top	5A	84	26.950 ± 541	35±1	144.4 ± 2.1	0.6777 ± 0.0029	95 378±711	$87\ 227\pm5826$	185 ± 4.0	$84\ 162\pm5826$
BR 2 top	5B	75	9403 ± 189	87±2	149.7 ± 2.1	0.6617 ± 0.0026	$91\ 172\pm618$	$88\ 052\pm2289$	192 ± 2.9	87 978±2289
BR 2 bottom	6A	68	7334 ± 148	131 ± 3	145.3 ± 2.1	0.6576 ± 0.0023	$90\ 917\pm567$	88 868±1552	187 ± 2.8	88 803±1552
BR 2 bottom	6B	68	6498 ± 130	149±3	146.5 ± 1.6	0.6576 ± 0.0021	90 748±500	88951 ± 1363	188 ± 2.2	88 887±1363
BR3 Top big	14	181	$21\ 239\pm428$	106 ± 2	177.6 ± 2.1	0.7560 ± 0.0027	$108\ 039\pm732$	$105\ 253\pm2096$	239 ± 3.0	$105\ 118\pm2096$
BR3 Top big	11B	180	$10\ 042\pm202$	200±4	179.9 ± 2.1	0.6791 ± 0.0023	90 822±548	$89\ 494\pm1084$	232 ± 3.0	$89\ 429\pm1084$
BR3 Top small	2A	119	39 624±797	36 ± 1	144.7 ± 2.1	0.7263 ± 0.0032	$106\ 550\pm 859$	$98\ 117\pm6042$	191 ± 4.0	$98\ 052\pm6042$
BR3 Top small	2B	116	29 348±590	47±1	157.3 ± 2.0	0.7146 ± 0.0028	101 698±716	95 434±4493	206 ± 4.0	95 369±4493
BR 3 bottom small	3A	85	$32\ 394\pm650$	31 ± 1	157.8 ± 2.0	0.7228 ± 0.0028	$103\ 518\pm720$	6089∓066 €6	206 ± 4.7	93 925 \pm 6809
BR 3 bottom small	3B	82	$12\ 161\pm 244$	78±2	155.4 ± 2.0	0.7017 ± 0.0023	965∓080 66	$95\ 443\pm2639$	203 ± 3.1	95 378 \pm 2639
BR 3 bottom big	4A	48	10 654 ± 214	53±1	164.3 ± 1.9	0.7216 ± 0.0028	$102\ 216\pm716$	96731 ± 3948	216 ± 3.5	96 666±3948
BR 3 bottom big	4B	47	9754 + 196	56+1	161.2 + 2.1	0.7148 ± 0.0028	101 154+727	96.025 ± 3700	211 + 3.6	95.960 + 3700

axis, the halved samples display small cavities and discontinuities. The growth axis clearly shifted with time as the drip point moved laterally, giving rise to an asymmetrical stalagmite so that only one flank of the underlying edifice was partially coated (Fig. 3).

Sample BR2 is approximately 28 cm in height and ranges from 8 to 10 cm in diameter. The shape is a nearly symmetrical candle with a larger diameter in the middle part. Compared to BR1, the yellowish-grey BR2 exhibits darker colours on its weathered outer surface. The surface texture is irregular, rough and has some visible macro-holes at the bottom (Fig. 2A). The cut sample shows growth layers with darker bands interlayered with lighter bands. There are several obvious discontinuities (hiatus; Fig. 3).

Sample BR3 is significantly different from BR1 and BR2 in shape. It incorporates a smaller stalagmite in its lower portion. The length of the outer stalagmite is 36 cm and the diameter 8–11 cm. The inner stalagmite has a length of 26 cm and a diameter of 3–6 cm. Both stalagmites have an asymmetrical shape with the smallest diameter in their middle. The growth layers and growth axis of the inner stalagmite are unlike the outer one (Fig. 3). The boundary between the stalagmites is characterized by a discontinuity. The porosity is high on the flanks of the two stalagmites.

In Fig. 3, CT images are displayed in greyscale. Lighter greyscale values indicate higher densities. Lower densities are observed in areas with high porosity or a hiatus (Fig. 3). The cut samples of BR1 and BR3 show axis holes (diameter >1 mm) extending parallel to the growth axis (Fig. 4). The axis holes were also previously observed in CT scan images of uncut samples (Fig. 3). This feature can

be caused by an elongated dissolution process that affects the primary porosity of columnar calcite and is initiated particularly as elongated cavities along the boundaries between neighbouring crystals (Perrin et al. 2014). The dissolution process gradually enlarges secondary voids. Their width varies from a few micrometres to a few hundreds of micrometres. In the last stage, these dissolution cavities become connected to each other and form a framework of micro-holes in the central part of the stalagmite (Perrin et al. 2014). The cut sample of BR2 shows its central voids with depressions downward across the layers (Fig. 4), where the CT image indicates lower densities. This feature may be caused by undersaturated or corrosive water cutting through the growth layers along micro-fractures inside (Shtober-Zisu et al. 2014).

The internal dissolution feature and shift of growth axis suggest that the samples BR1, BR2 and BR3 have suffered significant depositional changes during or after their growths. These changes however cannot be readily predicted from the uncut stalagmites. The CT images conversely reveal that the samples have significant density variations and contain small and large voids (Fig. 3). Obviously, the CT images provide unique information about the internal structure of stalagmites that cannot be identified by visual inspection of the uncut specimens (Figs 2B, 3).

Petrography and density

Petrographic analysis of polished thin sections can facilitate the identification of different types of calcite fabrics in the stalagmites (Frisia 2015). We prepared 19



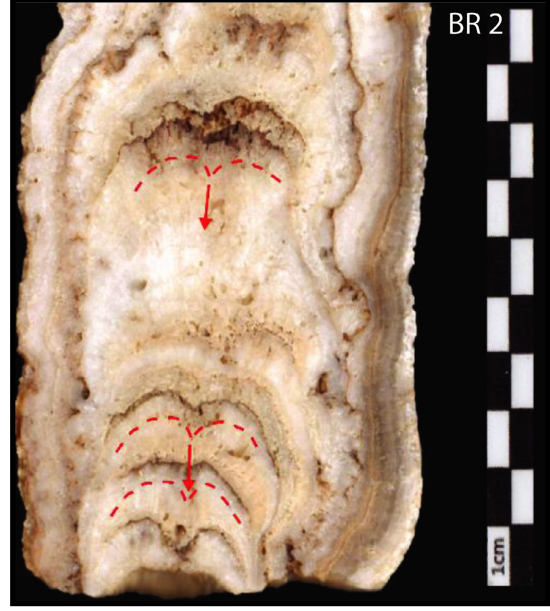
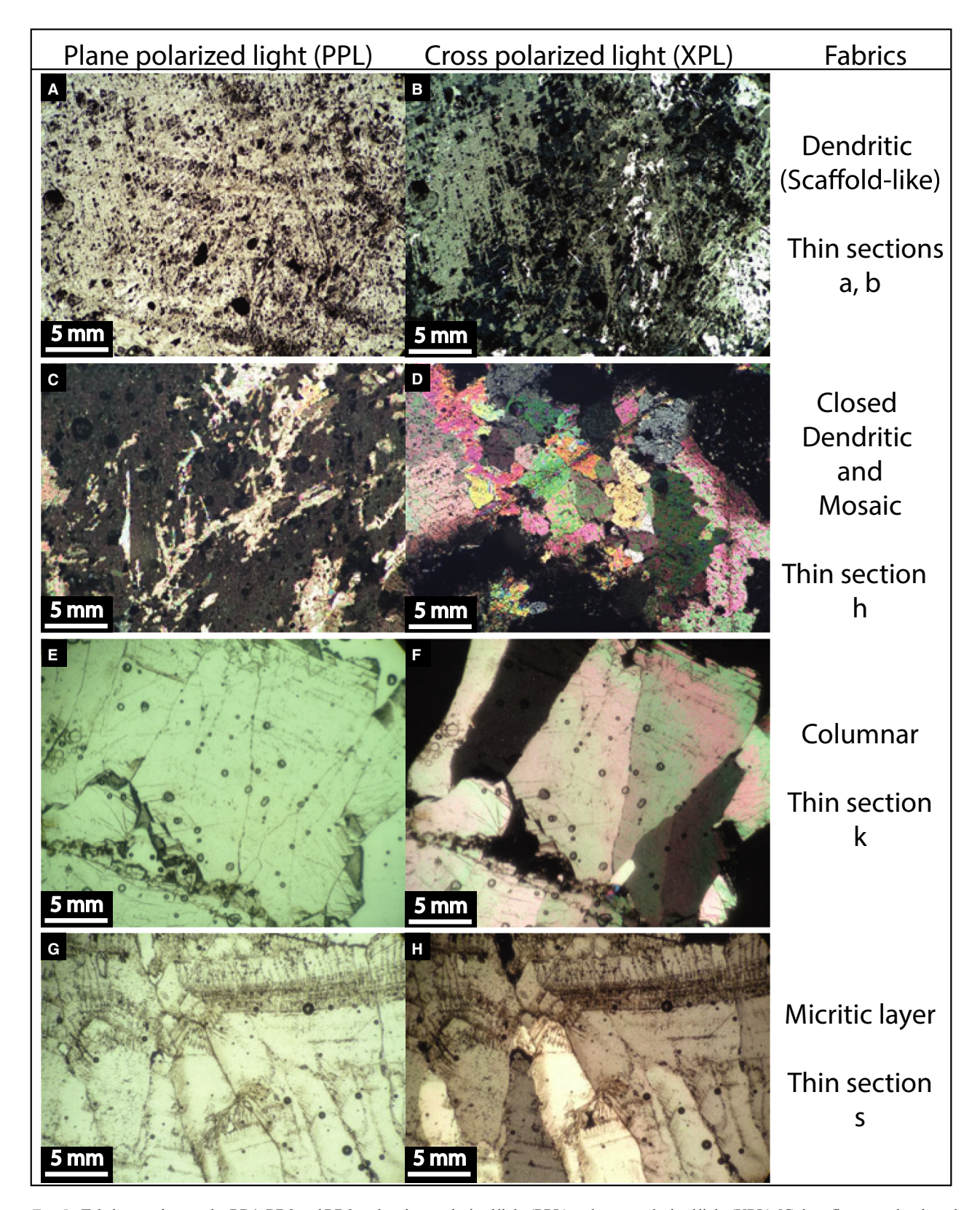


Fig. 4. Samples BR1 and BR2 showing axis holes elongated parallel to the growth axis with diameter ranging from 1 to 5 mm. In BR2, the marked feature shows downward bending of growth layers towards the holes. [Colour figure can be viewed at www.boreas.dk]



 $\textit{Fig. 5.} \ \ Fabric types in samples BR1, BR2 and BR3 under plane polarized light (PPL) and cross-polarized light (XPL). [Colour figure can be viewed at www.boreas.dk]$

This study		Vanghi et al.	(2015)	Walczak et a	ul. (2015) and Frisia (2015))	
HU values	Fabrics	HU values	Fabrics	HU values	Fabrics	Growth rate	Drip rate
<1200	Open dendritic	<226	Porous	<2000	Columnar microcrystalline, dendritic	Fast	Not stable and seasonally variable
		227–776	Dendritic				
1200-1400	Closed dendritic	77–1176	Closed dendritic				
1401-1550	Columnar	1177–1576	Columnar				
		1577–3071	Micrite	2000-2400	Open columnar	Medium	Constant with high drip rate
				>2400	Compacted columnar	Slow	Constant with low drip rate

Table 2. Characteristics of CT number (HU values), petrography, and palaeoenvironment of stalagmites.

polished thin sections from samples BR1, BR2 and BR3. Four fabric types can be observed (Fig. 5A–H, see positions of polished thin sections in Fig. 3). (i) Open dendritic fabric formed interlocking and elongated crystals. This texture is characterized by high porosity (Frisia *et al.* 2000, 2002). (ii) Closed dendritic fabric has more equal dimensions and forms fewer porous laminae. (iii) Columnar fabric is characterized by large crystals growing parallel to the central axis. Their crystal boundaries are acute. In general, the columnar fabric is less porous than the dendritic fabric (Frisia 2015). (iv) Micritic layers are observed mainly on the edges of the stalagmite BR3.

In this study, variations in the crystalline fabric as well as the porosities are represented in the CT numbers (HU) in Table 2. The open dendritic fabric shows a high porosity with the lowest density (<1200 HU). Closed dendritic fabric has a medium density (1200–1400 HU). Columnar fabric has the highest density (1401–1550 HU). The calcite fabrics and CT numbers (HU) of Tham Nam stalagmites were then compared to those previously reported in Vanghi et al. (2015), Walczak et al. (2015) and Frisia (2015) (Table 2). Stalagmites BR1, BR2 and BR3 display CT numbers (HU) <1550, and fabrics indicate variable drip rates and fast growth rates (Frisia 2015). Density in a speleothem is related to primary crystalline texture and porosity. Secondary porosity can be the result of dissolution and/or fractures that lead to lower density. Diagenesis can cause loss of primary texture, mineralogy and geochemical signatures (Perrin et al. 2014; Scholz et al. 2014; Zhang et al. 2014; Bajo et al. 2016). Thus, the present work, in agreement with previous studies (Vanghi et al. 2015; Walczak et al. 2015), suggests that the areas within stalagmites regarded suitable for palaeoclimatic study should exhibit primary crystalline texture, low porosity and CT numbers (HU) of 1550 or higher.

U-Th dating

All U-Th ages of the subsamples from stalagmites BR1, BR2 and BR3 are replicable within uncertainties, except

for 1A and 1B (Table 1; Fig. 3). In fact, in each pair of replicates, the difference between the mean ages is much smaller than the uncertainty (2σ) , which suggests that the U-Th chemical separations and machine measurements are robust. The measured ²³⁸U concentrations and δ^{234} U values can also be well replicated. However, the ²³²Th content and values of the ²³⁰Th/²³²Th atomic ratio show considerable variation. This Th heterogeneity is probably due to an uneven distribution of detritus, which contains high Th contents. The discrepancy in U-Th ages between subsamples 1A and 1B near the top layer of stalagmite BR3 is probably caused by a diagenetic process (e.g. dissolution, recrystallization and neomorphism) because they were drilled in the low-density part of the sample (Fig. 3).

(Fig. 3).

238 U concentrations in all the samples are lower than 200 ppb and ²³²Th concentrations range from thousands to tens of thousands of ppt. The isotopic ratios of ²³⁰Th to ²³²Th are also low, typically <200 ppm. This unfortunately limits the age precisions, which largely depend on the ²³⁰Th initial correction. A low ²³⁸U concentration and particularly low ²³⁰Th/²³²Th values indicate that a significant portion of ²³⁰Th does not originate from *in situ* decay of ²³⁸U. The large uncertainty of the detrital ²³⁰Th/²³²Th in bulk earth values thus dominates the age uncertainties. Nevertheless, if the ²³²Th concentration in the subsample is low and the measured ²³⁰Th/²³²Th value is high, the relative uncertainty of the corrected age can easily be reduced to $\sim 1\%$ or better (e.g. BR1 bottom (8B), Table 1). After the initial Th correction, all the U-Th ages of BR1, BR2 and BR3 are concentrated in a small interval, ranging between 87 and 105 ka. This confirms that they were deposited during the same time interval.

CT images, petrography and U-Th isotope data indicate the dissolution features in the internal structure of stalagmites BR1, BR2 and BR3. These can be caused by several scenarios, for example, (i) undersaturated or acidic dripping water with high content of pCO₂ (Perrin et al. 2014); (ii) an abruptly increasing dripping water rate, which prevents sufficient degassing to bring feeding water to equilibrium with CaCO₃ (Railsback et al. 2011);

or (iii) mixing of dissolution solution with several drip water sources (Scholz et al. 2014). Recent studies suggest that microbial activity can affect calcification through trapping and binding detrital particles and inducing calcite precipitation. This leads to breakdown dissolution, boring and residue micrite production (Jones 2001; Shtober-Zisu et al. 2014). Such processes can change the primary isotopic and elemental composition of a speleothem. These changes alter the geochemical signals, which may have an impact on the interpretation of the results obtained in palaeoenvironmental studies (Martín-García et al. 2009). Typically, stalagmite samples containing these features are no longer suitable for palaeoclimate studies. For speleothem age determination, carbonate samples must have remained completely closed with respect to loss or gain of U and Th isotopes. For example, Bajo et al. (2016) reported that U-Th ages could be overestimated in a stalagmite that has anomalously high ²³⁰Th/²³⁸U isotopic ratios resulting from preferential U loss in micro-void dissolution. Based on the CT images, petrography analysis and large uncertainty of ²³⁰Th/²³²Th, we hereby decided not to perform any additional dating and geochemical analysis on the stalagmites from Tham Nam cave.

Conclusions

In the present work, stalagmites from Tham Nam cave, western Thailand, were evaluated for their palaeoclimatic research potential, through X-ray computed tomography (CT scanning), petrography, and U-Th dating analysis. The CT scanning data reveal that stalagmite density is associated with fabrics and distribution of porosity. The porosity/axis-holes/voids in the stalagmites are related to postdepositional dissolution processes and may have an influence on U-Th dating accuracy. The ages of stalagmites from the Tham Nam Cave range between 87 and 105 ka. Currently, they are the oldest stalagmites that have been reported from mainland Southeast Asia. However, the stalagmites show dissolution features, several discontinuities and large age uncertainty, and are thus probably not suitable for palaeoclimatic research. Consistent with previous work (Mickler et al. 2004a, b; Zisu et al. 2012; Vanghi et al. 2015; Walczak et al. 2015 and Bajo et al. 2016), this study suggests that CT images have a large yet underestimated potential in speleothem study. They can help to identify internal structures in samples that may compromise geochemical elemental and isotopic analyses. For stalagmites potentially suitable for palaeoenvironmental research, CT scanning can also facilitate selection of the right cutting location. This study hence sets an example for future speleothem exploration using CT scanning as a tool to examine petrological textures prior to any further analysis.

Acknowledgements. – S. Chawchai wishes to express appreciation for the financial support provided by the Ratchadaphiseksomphot Endowment Fund, part of the 'Research Grant for New Scholar CU Researcher's

Project', DPST and the Thailand Research Fund (MRG5980080). X.W. is supported by a Singapore National Research Foundation (NRR) Fellowship (NRFF2011-08). The authors would also like to thank Mr. Siripong Tonongto, his family and PANDA CAMP for accommodation and assistance during the field survey. In addition, the authors want to thank Peerapong Sritangsirikul and officials at Ban Rai district, Uthai Thani province, for their help and hospitality as well as Dr. Thanisa Tongbai (Diagnostic Radiologist) and Walaiporn Suksancharoen (nurse) at King Chulalongkorn Memorial Hospital for their advice and help. We also thank the editor and anonymous reviewers for their careful reading of our manuscript and their insightful comments and suggestions.

References

- Bajo, P., Hellstrom, J., Frisia, S., Drysdale, R., Black, J., Woodhead, J.,
 Borsato, A., Zanchetta, G., Wallace, M. W., Regattieri, E. & Haese, F.
 2016: "Cryptic" diagenesis and its implications for speleothem geochronologies. *Quaternary Science Reviews* 148, 17–28.
- Cai, B., Pumijumnong, N., Tan, M., Muangsong, C., Kong, X., Jiang, X. & Nan, S. 2010: Effects of intraseasonal variation of summer monsoon rainfall on stable isotope and growth rate of a stalagmite from northwestern Thailand. *Journal of Geophysical Research: Atmospheres* 115, D21104, https://doi.org/10.1029/2009JD013378.
- Chen, F., Xu, Q., Chen, J., Birks, H. J. B., Liu, J., Zhang, S., Jin, L., An, C., Telford, R. J., Cao, X., Wang, Z., Zhang, X., Selvaraj, K., Lu, H., Li, Y., Zheng, Z., Wang, H., Zhou, A., Dong, G., Zhang, J., Huang, X., Bloemendal, J. & Rao, Z. 2015: East Asian summer monsoon precipitation variability since the last deglaciation. *Scientific Reports* 5, 11186, https://doi.org/10.1038/srep11186.
- Cheng, H., Edwards, R. L., Shen, C. C., Polyak, V. J., Asmerom, Y., Woodhead, J., Hellstrom, J., Wang, Y., Kong, X., Spötl, C., Wang, X. & Calvin Alexander, E. Jr. 2013: Improvements in ²³⁰Th dating, ²³⁰Th and ²³⁴U half-life values, and U-Th isotopic measurements by multicollector inductively coupled plasma mass spectrometry. *Earth and Planetary Science Letters* 371, 82–91.
- Cook, E. R., Anchukaitis, K. J., Buckley, B. M., D'Arrigo, R. D., Jacoby, G. C. & Wright, W. E. 2010: Asian monsoon failure and mega drought during the last millennium. *Science* 328, 486–489.
- Department of Mineral Resources (DMR) 2009: Geological Map of Thailand (Uthai Thani) Scale 1: 250000. Ministry of Natural Resource and Environment, Bangkok, Thailand.
- Edwards, R. L., Chen, J. H. & Wasserburg, G. J. 1986: ²³⁸U-²³⁴U-²³⁰Th-²³²Th systematics and the precise measurement of time over the past 500,000 years. *Earth and Planetary Science Letters 81*, 175-192
- Fairchild, I. J. & Treble, P. C. 2009: Trace elements in speleothems as recorders of environmental change. *Quaternary Science Reviews* 28, 449–468.
- Fairchild, I. J., Smith, C. L., Baker, A., Fuller, L., Spötl, C., Mattey, D. & McDermott, F. 2006: Modification and preservation of environmental signals in speleothems. *Earth-Science Reviews* 75, 105–153.
- Frisia, S. 2015: Microstratigraphic logging of calcite fabrics in speleothems as tool for palaeoclimate studies. *International Journal of Speleology* 44, 1–16.
- Frisia, S., Borsato, A., Fairchild, I. J. & McDermott, F. 2000: Calcite fabrics, growth mechanisms, and environments of formation in speleothems from the Italian Alps and Southwestern Ireland. *Journal of Sedimentary Research* 70, 1183–1196.
- Frisia, S., Borsato, A., Fairchild, I. J., McDermott, F. & Selmo, E. M. 2002: Aragonite-calcite relationships in speleothems (Grotte de Clamouse, France): environment, fabrics, and carbonate geochemistry. *Journal of Sedimentary Research* 72, 687–699.
- Hendy, C. H. 1971: The isotopic geochemistry of speleothems—I. The calculation of the effects of different modes of formation on the isotopic composition of speleothems and their applicability as palaeoclimatic indicators. *Geochimica et Cosmochimica Acta 35*, 801–824.

- Jaffey, A. H., Flynn, K. F., Glendenin, L. E., Bentley, W. T. & Essling, A. M. 1971: Precision measurement of half-lives and specific activities of ²³⁵U and ²³⁸U. *Physical Review C4*, 1889.
- Jones, B. 2001: Microbial activity in caves—a geological perspective. Geomicrobiology Journal 18, 345–357.
- Ketcham, R. A. & Carlson, W. D. 2001: Acquisition, optimization and interpretation of X-ray computed tomographic imagery: applications to the geosciences. *Computers and Geosciences* 27, 381–400.
- Lachniet, M. S. 2009: Climatic and environmental controls on speleothem oxygen-isotope values. *Quaternary Science Reviews* 28, 412–432
- Loo, Y. Y., Billa, L. & Singh, A. 2015: Effect of climate change on seasonal monsoon in Asia and its impact on the variability of monsoon rainfall in Southeast Asia. Geoscience Frontiers 6, 817–823.
- Martín-García, R., Alonso-Zarza, A. M. & Martín-Pérez, A. 2009: Loss of primary texture and geochemical signatures in speleothems due to diagenesis: evidences from Castañar Cave, Spain. Sedimentary Geology 221, 141–149.
- McDermott, F. 2004: Palaeo-climate reconstruction from stable isotope variations in speleothems: a review. *Quaternary Science Reviews 23*, 901–918.
- Mickler, P. J., Banner, J. L., Stern, L., Asmerom, Y., Edwards, R. L. & Ito, E. 2004b: Stable isotope variations in modern tropical speleothems: evaluating equilibrium vs. kinetic isotope effects. *Geochimica et Cosmochimica Acta* 68, 4381–4393.
- Mickler, P. J., Ketcham, R. A., Colbert, M. W. & Banner, J. L. 2004a: Application of high-resolution X-ray computed tomography in determining the suitability of speleothems for use in palaeoclimatic, palaeohydrologic reconstructions. *Journal of Cave and Karst Studies* 66, 3–8.
- Muangsong, C., Cai, B., Pumijumnong, N., Hu, C. & Cheng, H. 2014: An annually laminated stalagmite record of the changes in Thailand monsoon rainfall over the past 387 years and its relationship to IOD and ENSO. *Quaternary International 349*, 90–97.
- Perrin, C., Prestimonaco, L., Servelle, G., Tilhac, R., Maury, M. & Cabrol, P. 2014: Aragonite-calcite speleothems: identifying original and diagenetic features. *Journal of Sedimentary Research* 84, 245–269.
- Raghavan, S. V., Liu, J., Nguyen, N. S., Vu, M. T. & Liong, S. Y. 2017: Assessment of CMIP5 historical simulations of rainfall over Southeast Asia. *Theoretical and Applied Climatology*, 1–14, https://doi.org/10.1007/s00704-017-2111-z.
- Railsback, L. B., Dabous, A. A., Osmond, J. K. & Fleisher, C. J. 2002: Petrographic and geochemical screening of speleothems for U-series dating: an example from recrystallized speleothems from Wadi Sannur Cavern, Egypt. *Journal of Cave and Karst Studies* 64, 108–116.
- Railsback, L. B., Liang, F., Romaní, J. R. V., Grandal-d'Anglade, A., Rodríguez, M. V., Fidalgo, L. S., Mosquera, D. F., Cheng, H. & Edwards, R. L. 2011: Petrographic and isotopic evidence for Holocene long-term climate change and shorter-term environmental

- shifts from a stalagmite from the Serra do Courel of northwestern Spain, and implications for climatic history across Europe and the Mediterranean. *Palaeogeography, Palaeoclimatology, Palaeoecology* 305, 172–184.
- Scholz, D., Tolzmann, J., Hoffmann, D. L., Jochum, K. P., Spötl, C. & Riechelmann, D. F. 2014: Diagenesis of speleothems and its effect on the accuracy of ²³⁰Th/U-ages. *Chemical Geology 387*, 74–86.
- Shen, C. C., Wu, C. C., Cheng, H., Edwards, R. L., Hsieh, Y. T., Gallet, S., Chang, C.-C., Li, T.-Y., Lam, D. D., Kano, A., Hori, M. & Spötl, C. 2012: High-precision and high-resolution carbonate 230Th dating by MC-ICP-MS with SEM protocols. *Geochimica et Cosmochimica Acta* 99, 71–86.
- Shtober-Zisu, N., Schwarcz, H. P., Chow, T., Omelon, C. R. & Southam, G. 2014: Caves in caves: evolution of post-depositional macroholes in stalagmites. *International Journal of Speleology* 43, 323–334.
- Sinha, A., Kathayat, G., Cheng, H., Breitenbach, S. F., Berkelhammer, M., Mudelsee, M., Biswas, J. & Edwards, R. L. 2015: Trends and oscillations in the Indian summer monsoon rainfall over the last two millennia. *Nature Communications* 6, https://doi.org/10.1038/nc omms7309.
- Thirumalai, K., DiNezio, P. N., Okumura, Y. & Deser, C. 2017: Extreme temperatures in Southeast Asia caused by El Niño and worsened by global warming. *Nature Communications* 8, https://doi.org/10.1038/ncomms15531.
- Vanghi, V., Iriarte, E. & Aranburu, A. 2015: High resolution X-ray computed tomography for petrological characterization of speleothems. *Journal of Cave and Karst Studies* 77, 75–82.
- Walczak, I. W., Baldini, J. U., Baldini, L. M., McDermott, F., Marsden, S., Standish, C. D., Richards, D. A., Andreo, B. & Slater, J. 2015: Reconstructing high-resolution climate using CT scanning of unsectioned stalagmites: a case study identifying the mid-Holocene onset of the Mediterranean climate in southern Iberia. *Quaternary Science Reviews* 127, 117–128.
- Wong, C. I. & Breecker, D. O. 2015: Advancements in the use of speleothems as climate archives. *Quaternary Science Reviews* 127, 1–18.
- Zhang, H., Cai, Y., Tan, L., Qin, S. & An, Z. 2014: Stable isotope composition alteration produced by the aragonite-to-calcite transformation in speleothems and implications for palaeoclimate reconstructions. *Sedimentary Geology* 309, 1–14.
- Zhang, P., Cheng, H., Edwards, R. L., Chen, F., Wang, Y., Yang, X., Liu, J., An, C., Dai, Z., Zhou, J., Zhang, D., Jia, J., Jin, L. & Johnson, R. K. 2008: A test of climate, sun, and culture relationships from an 1810-year Chinese cave record. *Science 322*, 940–942.
- Zisu, N. S., Schwarcz, H. P., Konyer, N., Chow, T. & Noseworthy, M. D. 2012: Macroholes in stalagmites and the search for lost water. *Journal of Geophysical Research: Earth Surface 117*, F03020, https://doi.org/10.1029/2012JF002619.